Applied Energy 333 (2023) 120569

Contents lists available at ScienceDirect

Applied Energy

journal homepage: www.elsevier.com/locate/apenergy

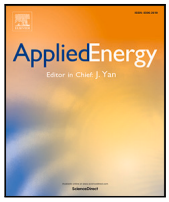

Optimal scheduling of multi-energy type virtual energy storage system in reconfigurable distribution networks for congestion management

Farid Hamzeh Aghdam [a], Manthila Wijesooriya Mudiyanselage [c], Behnam Mohammadi-Ivatloo [a,b], Mousa Marzband [c,d,*]

[a] Faculty of Electrical and Computer Engineering, University of Tabriz, Tabriz, Iran
[b] Information Technologies Application and Research Center, Istanbul Ticaret University, Istanbul, Turkey
[c] Northumbria University, Electrical Power and Control Systems Research Group, Ellison Place NE1 8ST, Newcastle upon Tyne, UK
[d] Center of Research Excellence in Renewable Energy and Power Systems, King Abdulaziz University, Jeddah, 21589, Saudi Arabia

ARTICLE INFO

Keywords:
Virtual energy storage system
Congestion management
Bi-level formulation
Multi-carrier energy system

ABSTRACT

The virtual energy storage system (VESS) is one of the emerging novel concepts among current energy storage systems (ESSs) due to the high effectiveness and reliability. In fact, VESS could store surplus energy and inject the energy during the shortages, at high power with larger capacities, compared to the conventional ESSs in smart grids. This study investigates the optimal operation of a multi-carrier VESS, including batteries, thermal energy storage (TES) systems, power to hydrogen (P2H) and hydrogen to power (H2P) technologies in hydrogen storage systems (HSS), and electric vehicles (EVs) in dynamic ESS. Further, demand response program (DRP) for electrical and thermal loads has been considered as a tool of VESS due to the similar behavior of physical ESS. In the market, three participants have considered such as electrical, thermal and hydrogen markets. In addition, the price uncertainties were calculated by means of scenarios as in stochastic programming, while the optimization process and the operational constraints were considered to calculate the operational costs in different ESSs. However, congestion in the power systems is often occurred due to the extreme load increments. Hence, this study proposes a bi-level formulation system, where independent system operators (ISO) manage the congestion in the upper level, while VESS operators deal with the financial goals in the lower level. Moreover, four case studies have considered to observe the effectiveness of each storage system and the simulation was modeled in the IEEE 33-bus system with CPLEX in GAMS.

1. Introduction

Over the past decades, innovative power system technologies have been integrated significantly with smart grids to overcome the burden of environmental impacts and carbon emissions. Thus, the future power systems would be more efficient and sustainable with renewable energy sources (RESs), such as photovoltaic systems and wind turbines. However, the intermittent nature of RESs leads to unbalance in the power supply and demand with insecure and instable system. Although fossil fuel generators are comparatively more stable than RESs generators, carbon emission and noise pollution make them less attractive [1]. Hence, more attention was obtained by energy storage systems (ESSSs) due to compensation of the uncertainty associated with the RES and storing/releasing the energy according to the system requirements. In the presence of the uncertain power supply, ESS could guarantee a stable power system while enhancing the system efficiency [2]. ESS could facilitate the following possibilities in terms of generator's and consumer's point of view:

- Transferring generation capacity from peak hours to off peak hours to benefit the generation units
- Compensating generation uncertainty to facilitate the application of RES.
- Encouraging the customers to shift peak hour consumption to off-peak times while altering the consumer habits.

Various forms of ESSs are available at the current market such as electrochemical (e.g. batteries), mechanical (e.g. flywheels), electrical (e.g. super capacitors) and thermal systems (e.g. hot water storage) [1]. Although, in recent years many technologies have been introduced to reduce the cost of ESSs, they are still one of the most expensive units in energy systems. Thus, these systems could be critical to encourage the private sector to invest. The progress in technology and tendency to reduce emissions, have attracted the smart grid developers to apply novel technologies for ESS beside conventional battery ESSs (BESSs), e.g. power-to-X (P2X) and X2P technologies. In this regard,

* Corresponding author at: Northumbria University, Electrical Power and Control Systems Research Group, Ellison Place NE1 8ST, Newcastle upon Tyne, UK.
E-mail address: mousa.marzband@northumbria.ac.uk (M. Marzband).

https://doi.org/10.1016/j.apenergy.2022.120569
Received 20 September 2022; Received in revised form 29 November 2022; Accepted 20 December 2022
Available online 2 January 2023

hydrogen-based power technologies, such as power-to-hydrogen (P2H) and hydrogen-to-power (H2P), are one of promising methods for zero emission networks. Fuel cells can be used for H2P purposes where hydrogen and oxygen reactions produce electricity, heat, and water [2]. In fact, the electrolyzer is used to decompose the exhausting water of the fuel cell into hydrogen and oxygen and then store in storage tanks [3]. The produced hydrogen could be utilized to produce electricity or can be sold to hydrogen market specially for hydrogen vehicles (which have clean output with the low-carbon policies) [4]. In particular, the energy of 1 kg of hydrogen fuel equals to energy of 2.8 kg of oil or 2.1 kg of natural gas, which shows that hydrogen has the highest energy density per unit of mass between other energy carriers. Consequently, hydrogen is renewable and environmental-friendly [5].

In modern energy systems, combined heat and power (CHP) units are another power generation methods because of their effective contribution to electrical and thermal energy supply, and the waste produced of this system is used to fulfill heating loads. Applying fuel cells as CHPs, can be encountered as a highly efficient combination of energy technologies in recent years [6,7]. On the other hand, thermal storage systems (TES) are usually used beside the CHPs to compensate their insufficiency, which is due to interdependency between the electrical and thermal energies of CHPs.

Electrical vehicles (EVs) are one of the alternatives for conventional transportation systems. In fact, EVs not only participate in low-carbon policies, but also include several batteries, which could utilize as non-stationary ESS to store electrical energy and perform the vehicle-to-grid (V2G) actions. Accordingly, EVs can contribute to the environment-friendly, reliable and flexible performance of the energy systems [4, 8].

A virtual energy storage system (VESS) aggregates various controllable elements of energy systems, to store the surplus power or inject the shortage amount according to the system requirements [9]. In other words, a VESS is operated as a single high capacity and high power ESS, which is appropriate for smart grids. Further, the VESS could be considered as a shared energy storage that provides ESS services to small scale users. Thus, by introducing VESS, small and various capacity ESSs, can get access to the wholesale market. The unit price of the system could reduce by installing VESS, where the installation cost of ESS is comparatively high. Moreover, utilization of VESSs can gain many advantages such as integrating the RES in the distribution networks, reducing network expansion, decreasing generation margins and the required spinning reserve capacity along with providing ancillary services to the network [10]. Customers participating in the VESS, VESS could rent the ESS capacity they require and decide the charging and discharging status as an individual ESS. Furthermore, the VESS operator performs a centralized action for its elements in order to provide the customer demand/supply level [11]. Demand response programs (DRPs) could also play as VESS due to smart managing of energy consumption. This can be inferred by using more energy as in charging mode and reducing the demand level during the discharging period. Hence, DRPs in VESSs could be a cost effective option compared to the physical ESSs. Fig. 1 demonstrates a typical VESS structure with various types of ESSs and responsive loads.

Electrical power system industry is restructuring due to the participation of private sector investors instead of government investors to answer the growing demand of electricity around the world [12]. However, this increment in both demand and supply sides can lead to congestion in the network. Congestion refers to violating the thermal capacities of the lines, which hinders power delivery to the loads [13]. Independent system operator (ISO) could perform a congestion management by technical or non-technical methods, to control the congestion when delivering power. Technical methods include physical changes in the structure of the network, while non-technical approaches are performed using algorithmic methods such as market-based operations.

Decision making under certainty is difficult to define due to the unknown future parameters. One of the sources of uncertainty that could affect the financial aspects of a decision making process, is the price of trading commodities, which is the amount of traded energy in energy systems. Therefore, stochastic programming can be utilized for formulating and solving problems with uncertain parameters as random variables with known probability functions. An accurate list of market prices could be achieved by increasing the number of scenarios, and the calculation complexity could reduced by introducing scenario reduction methods such as fast-forward selection method. [14,15].

1.1. Research gap and contributions

1.1.1. Literature survey

A VESS is a combination of energy storage systems that are placed in different locations but managed by the VESS operator. Few studies have been dedicated to this field of research. Authors in [16], have proposed a two-stage optimization formulation for VESS operation. In the first stage, the aggregator of the ESSs determines the pricing of the storage and then in the second stage, each user of ESSs decides about the storage scheduling, while the batteries are considered as the only technology used in the VESS. A framework for real-time energy management is proposed in [17] based on the alternating direction method of multipliers (ADMM) as a distributed algorithm. Jin et al. [18], have suggested a building based VESS model by utilizing the heat storage of the building and considering a dynamic economic dispatch model for daily operating cost reduction. Authors in [19], have proposed an innovative and cost-effective VESS to charge and discharge according to the regulation signals. In this paper, the VESS is operated to provide frequency response with zero carbon policies instead of using the spinning reserve capacity of fossil-fuel generators. Wang et al. [20] have proposed a hierarchical dispatch strategy for VESSs, i.e., residential houses with air conditioners, which is introduced for voltage regulation in low-voltage networks with high penetration of solar systems. In [21], an operation strategy of a dynamic VESS for smart energy communities has been proposed. In the proposed method, the usage-limited constraint is considered to restrict the usage of various parts of VESS in the operation period. Moreover, a VESS-based energy management is proposed in [22] to enhance the availability of power supply. The VESS is composed of the high thermal inertia demands besides the batteries. Authors in [23], have presented optimal day-ahead scheduling for integrated energy system considering demand response, and VESS to maximize the overall benefits of units by game theory methodology. A risk-based VESS service strategy for prosumers is demonstrated in [11] to study the economic benefits and risks of increasing the capacity of the VESSs. Authors in [9] have investigated the role of VESS as a solution to convert to low carbon cities. Zhu et al. [24] have presented usage of EVs and heat storage of buildings, as a joint VESS system including electric and thermal energy storage systems. Furthermore, the research [25] has focused on power management and real-time control for VESS. A distributed multi-objective power management scheme is proposed to present competing objective functions where a Nash Bargaining Solution is used to find an optimal, unique and fair solution. A VESS-based structure is proposed in [26] for enhancing the scalability and flexibility of the system. The VESS is composed of batteries, and flexible loads. To obtain voltage regulation, a dynamic pricing strategy according to system voltage condition is proposed in this study. Niromandfam et al. [27] have proposed the utilization of demand response resources as a VESS to decrease/increase the consumption of some demands according to some incentives. This variations in demand level provide the same behavior as discharging/charging of a conventional ESS.

1.1.2. Contributions and paper structure

Numerous operational problems have been occured due to high penetration of RESs into energy systems, which can be handled by using of ESSs. In fact, VESSs could contain different types of ESSs and other flexible resources like flexible loads. However, an energy management

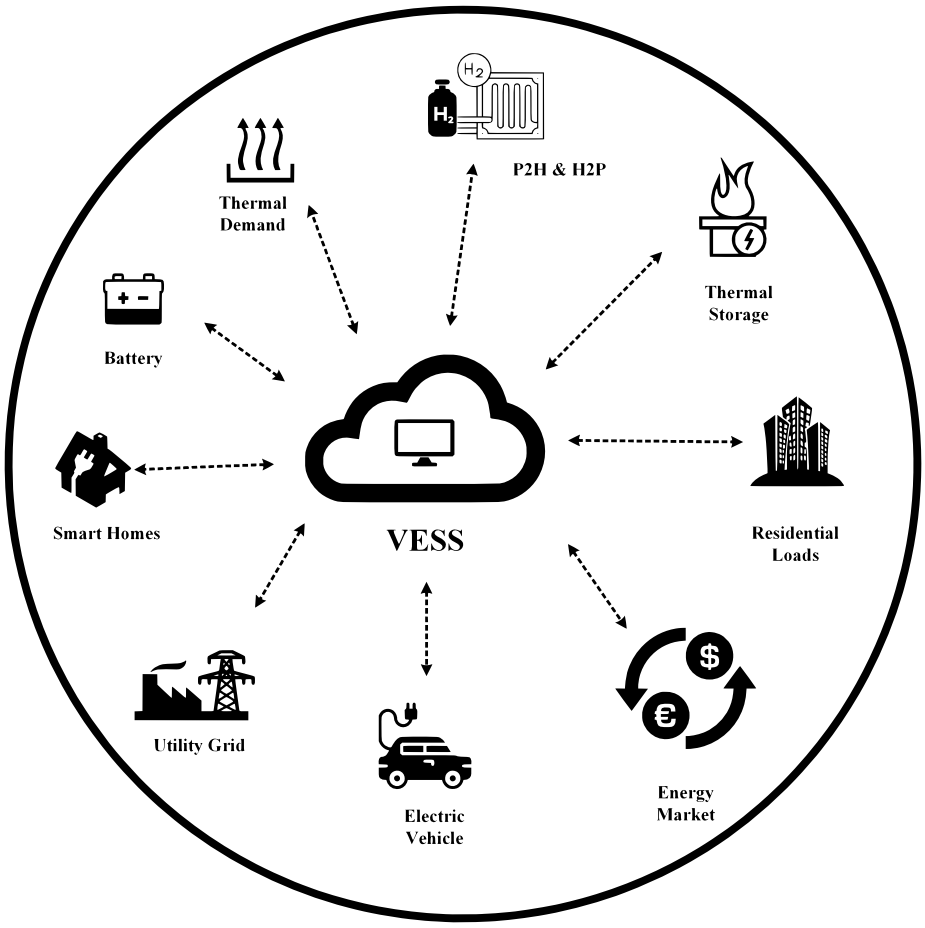

Fig. 1. A typical VESS structure with various types of ESSs and responsive loads.

system is required for optimal scheduling of ESSs to maximize the benefits of VESSs, considering operational constraints, costs of devices and uncertainties of energy prices. DRPs could be performed as a ESSs, and the overall VESS function could be investigated by considering the effect of responsive loads as a low investment tool. Further, multi carrier energy systems were introduced to enhance the system efficiency, where the electrical and thermal load is fulfilled by VESSs. H2P and P2H technologies have immensely contributed to the clean energy concept. Moreover, in modern power grids, EVs play a key role in line with low carbon policies and can be used as non-stationary ESSs in V2G/G2V modes. However, power system are facing technical issues due to their rapid expansion. Accordingly, it is vital to consider mainly the technical problems compared to financial goals. The following items show a summary of the research gaps that exist in the studied papers in the literature review section:

- Focusing more on the financial aspects rather than technical issues of the system for operation of VESSs.
- Failure to consider co-optimization of VESS operator and system operator to consider technical issues of the network.
- Lack of sources with the concentration in various energy sources especially hydrogen, as one of the promising clean sources of energy.
- Failure to focus on the mathematical modeling and linearization of the optimization in the operation of VESS operation to obtain global optimum.

According to the previous subsection and existing research gap, it is deduced that a few studies have been carried out on the concept of VESS. Considering the items as the research gap in the previous subsection, Table 1 illustrates the findings of this study in comparison with other works in the literature. Further, the congestion management with the financial desires of multi-carrier VESS owners has not been addressed before. In this study, the optimal operation of a VESS, including batteries, TES systems, P2H and H2P technologies with hydrogen storage systems (HSS), EVs and DRPs, is investigated. Participation of electrical, thermal and hydrogen markets were also considered. The uncertainties of energy prices would be modeled by means of scenarios as in stochastic programming, while the operational costs of different ESSs would be contemplated in the optimization process along with operational constraints. To handle the congestion issues, a bi-level formulation for the problem is proposed with ISO at the upper level trying to operate the network for congestion management and VESS operator in the lower level pursuing its financial goals. To sum up, the main contributions could be highlighted as follows:

- Proposing an optimal scheduling method for a multi-carrier VESS considering the degradation cost for participation in electrical, thermal and hydrogen markets.
- Proposing a co-optimization of ISO and VESS as bi-level modeling for scheduling as ISO in the upper level and VESS owner in the lower level to obtain congestion management for ISO and financial goals for VESS.
- Proposing different case studies in a network containing a VESS with various multi-carrier ESSs, e.g. batteries, TES, P2H and H2P in an HSS, EVs and finally, DRPs as a tool for VESS.
- Using linearized modeling for the problem to achieve global optimum.
- Using scenarios to evaluate the uncertainties of energy market prices.

Table 1
Comparison of the proposed method with different studies.

Reference	Storage type				DRP	Congestion management	Uncertainty	Financial/technical aspect	Problem model
	Battery	EV	HES	TES					
[11]	✓	–	–	–	–	–	–	Financial	CVaR-MILP
[16]	✓	–	–	–	–	–	–	Financial	Two Stage
[17]	✓	–	–	✓	–	–	✓	Financial	Distributed ADMM
[18]	✓	–	–	✓	–	–	–	Financial	MINLP
[20]	–	–	–	✓	✓	–	–	Technical	Hierarchical
[22]	✓	–		✓	✓	–	–	Financial	Heuristic
[23]	–	–		✓	✓	–	–	Financial	Cooperative game theory
[27]	✓	✓	–	–	✓	–	✓	Financial	Quadratic Programming
This study	✓	✓	✓	✓	✓	✓	✓	**Financial/Technical**	**Bilevel-MILP**

The paper is sectioned as follows: Section 2 demonstrates system modeling and problem formulation for the optimal scheduling process. Further, the simulation results and the effectiveness of the proposed method are discussed in Section 4, and finally summarized this study in conclusion.

2. System modeling and problem formulation

In this section, a bi-level formulation and system modeling for the congestion management in presence of VESS in distribution networks will be introduced. The VESS consists of various energy storage types including batteries, thermal energy storage systems, hydrogen storage systems, electrical vehicles and responsive loads. In the upper level of the bi-level formulation, the ISO tries to reduce the system congestion, whereas the financial benefits are calculated by VESS in the lower level.

2.1. Battery

The batteries are one of the most popular energy storage devices in power systems, and this section discusses the modeling of battery system. The constraints for charging and discharging power of the battery are shown in Eqs. (1)–(2), while the constraints for the state of charge (SoC) of the battery are expressed in terms of Eqs. (3)–(6) and the released power constraint is represented using Eq. (7). The battery operational cost is expressed by Eq. (8) where the costs of using battery is considered [28].

$$0 \le P^{b}_{ch,t,\omega} \le \frac{P^{b}_{max}}{\eta^{b}_{ch}} \quad \forall t,\omega \tag{1}$$

$$0 \le P^{b}_{dch,t,\omega} \le P^{b}_{max} \cdot \eta^{b}_{dch} \quad \forall t,\omega \tag{2}$$

$$SoC^{b}_{t,\omega} = SoC^{b}_{t-1,\omega} - \frac{1}{E^{b}_{max}}\left(\frac{1}{\eta^{b}_{dch}} \cdot P^{b}_{dch,t,\omega} - \eta^{b}_{ch} \cdot P^{bat}_{ch,t,\omega}\right) \quad \forall t,\omega \tag{3}$$

$$0 \le SoC^{b}_{t,\omega} \le 1 \quad \forall t,\omega \tag{4}$$

$$SoC^{b}_{t_0} = SoC^{b}_{init} \tag{5}$$

$$SoC^{b}_{t_{fin}} = SoC^{b}_{fin} \tag{6}$$

$$P^{b}_{t,\omega} = P^{b}_{ch,t,\omega} - P^{b}_{dch,t,\omega} \quad \forall t,\omega \tag{7}$$

$$Cost^{b}_{t,\omega} = \mathcal{A}^{b} \cdot \left[P^{b}_{ch,t,\omega} + P^{b}_{dch,t,\omega}\right] \quad \forall t,\omega \tag{8}$$

where $P^{b}_{ch,t,\omega}$, $P^{b}_{dch,t,\omega}$, $P^{b}_{t,\omega}$ and $SoC^{b}_{t,\omega}$ stand for charging, discharging, net power and state of charge of the battery b at time t and scenario ω. Further, η^{b}_{ch} and η^{b}_{dch} show the efficiency of charging and discharging of the battery. P^{b}_{max}, SoC^{b}_{init} and SoC^{b}_{fin} stand for maximum power capacity, initial and final energy levels of the battery, respectively. Moreover, $\mathcal{A}$ is the cost coefficients of battery degradation cost.

2.2. Electrical Vehicle (EV) parking lot

In this section, modeling for the EVs as mobile energy storage will be discussed. The Vehicle to Grid (V2G) option is defined to enable the EV owner to trade energy with the utility. VESS can aggregate EVs for participating in the day-ahead scheduling to gain benefit for the EVs as well as other entities. EVs should be charged/discharged according to the initial SoC, arrival time and departure time, and also power and energy capacities of the EVs. The maximum charge and discharge rates of EVs are expressed in terms of Eqs. (9)–(10). The SoC of the EV is calculated via Eqs. (11)–(14) [7]. Furthermore a cost for operation of the EV is considered, which is paid to the EV owner as a penalty for decreasing its lifespan and it is calculated via Eq. (16).

$$0 \le P^{EV}_{ch,t,\omega} \le \frac{P^{EV}_{max}}{\eta^{EV}_{ch}} \quad \forall t,\omega \tag{9}$$

$$0 \le P^{EV}_{dch,t,\omega} \le P^{EV}_{max} \cdot \eta^{EV}_{dch} \quad \forall t,\omega \tag{10}$$

$$SoC^{EV}_{t,\omega} = SoC^{EV}_{t-1,\omega} - \frac{1}{E^{EV}_{max}}\left(\cdot\frac{1}{\eta^{EV}_{dch}} \cdot P^{EV}_{dch,t,\omega} - \cdot\eta^{EV}_{ch} \cdot P^{bat}_{ch,t,\omega}\right) \quad \forall t,\omega \tag{11}$$

$$0 \le SoC^{EV}_{t,\omega} \le 1 \quad \forall t,\omega \tag{12}$$

$$SoC^{EV}_{arrival} = SoC^{EV}_{init} \tag{13}$$

$$SoC^{EV}_{departure} = SoC^{EV}_{fin} \tag{14}$$

$$P^{EV}_{t,\omega} = P^{EV}_{ch,t,\omega} - P^{EV}_{dch,t,\omega} \quad \forall t,\omega \tag{15}$$

$$Cost^{EV}_{t,\omega} = \mathcal{A}^{EV} \cdot \left[P^{EV}_{ch,t,\omega} + P^{EV}_{dch,t,\omega}\right] - \lambda^{e} \cdot [SoC^{EV}_{fin} - SoC^{EV}_{init}] \cdot P^{EV}_{max} \quad \forall t,\omega \tag{16}$$

where $P^{EV}_{ch,t}$, $P^{EV}_{dch,t}$, P^{EV}_{t} and SoC^{EV}_{t} and represent charging, discharging, net power, and state of charge of the EV at time t, respectively. η^{EV}_{ch} and η^{EV}_{dch} indicate efficiencies of EV charging and discharging. P^{EV}_{max}, SoC^{EV}_{init} and SoC^{EV}_{fin} are respective parameters for maximum power capacity, initial and final energy levels of the EV and, $\mathcal{A}$ is the cost of using the battery off the EVs.

2.3. Thermal energy storage system

One of the main components of the VESS is the thermal energy storage (TES) system. Eqs. (17) and (18) stand for the charging and discharging thermal power capacity of the TES, whereas the changes in energy level of the TES is calculated via Eqs. (19)–(22). In (23) the net amount of thermal power of the system is shown and the positive value indicates the charging mode while the negative value represents the discharging mode. Further, it contains a power to heat (P2HT) unit that generates thermal power by electrical energy, and the relations of P2HT unit is shown via Eqs. (24) and Eq. (25). The cost of TES operation, is a function of its usage, which is expressed via Eq. (26). $H^{tes}_{ch,t,\omega}$, $H^{tes}_{dch,t,\omega}$, and $H^{tes}_{t,\omega}$ represent charging, discharging, and net thermal power of the tes at time t and scenario ω, respectively. Also, $H^{p2ht}_{t,\omega}$ and $P^{p2ht}_{t,\omega}$ are generated thermal and consumed electrical power of the P2HT unit. η^{tes}_{loss}, η^{tes}_{ch}, η^{tes}_{dch} and η^{p2ht} indicate thermal efficiency of the TES

tank, efficiency of charging/discharging of thermal power in TES and efficiency of power to heat unit. H^{tes}_{max}, E^{tes}_{max} and E^{tes}_{min} show maximum thermal power, maximum and minimum energy of the TES. Initial and final energy levels in the TES is shown by E^{tes}_{int} and E^{tes}_{fin} and $\mathcal{A}$ is the cost of using TES.

$$0 \le H^{tes}_{ch,t,\omega} \le \frac{H^{tes}_{max}}{\eta^{tes}_{ch}} \quad \forall t,\omega \tag{17}$$

$$0 \le H^{tes}_{dch,t,\omega} \le H^{tes}_{max} \cdot \eta^{tes}_{dch} \quad \forall t,\omega \tag{18}$$

$$E^{tes}_{t,\omega} = E^{tes}_{t-1,\omega} \cdot (1-\eta^{tes}_{loss}) + (H^{tes}_{ch,t,\omega} \cdot \eta^{tes}_{ch} - \frac{H^{tes}_{dch,t,\omega}}{\eta^{tes}_{dch}}) \quad \forall t,\omega \tag{19}$$

$$E^{tes}_{min} \le E^{tes}_{t,\omega} \le E^{tes}_{max} \quad \forall t,\omega \tag{20}$$

$$E^{tes}_{t_0} = E^{tes}_{int} \tag{21}$$

$$E^{tes}_{t_f} = E^{tes}_{fin} \tag{22}$$

$$H^{tes}_{t,\omega} = H^{tes}_{ch,t,\omega} - H^{tes}_{dch,t,\omega} \quad \forall t,\omega \tag{23}$$

$$H^{p2ht}_{t,\omega} = P^{p2ht}_{t,\omega} \cdot \eta^{p2ht} \quad \forall t,\omega \tag{24}$$

$$0 \le H^{p2ht}_{t,\omega} \le H^{p2ht}_{max} \quad \forall t,\omega \tag{25}$$

$$Cost^{tes}_{t,\omega} = \mathcal{A}^{tes} \cdot [H^{tes}_{ch,t,\omega} + H^{tes}_{dch,t,\omega}] \quad \forall t,\omega \tag{26}$$

2.4. Hydrogen Storage System (HSS)

In this section, modeling of P2H and H2P in presence of HSS is presented. The electrolyzer converts the power to the hydrogen (H_2) by decomposing water. In addition, fuel cell consumes hydrogen to produce electrical and thermal power. The HSS is a buffer system between the electrolyzer and fuel cell. Eqs. (27) and (28) stand for the charging and discharging hydrogen amount of the HSS, while the changes in hydrogen level of the HSS is defined using Eqs. (29)–(32). Further, in Eq. (33) charging and discharging H_2 are combined to define a value for amount of H_2 transaction of the HSS. Negative values indicate discharge of H_2 and positive values stand for charging of H_2. Eq. (34) shows the total hydrogen consumption of fuel cell according to its electrical power output. The maximum electrical power generation of the fuel cell is given by Eq. (35), while Eq. (36) shows the emitted thermal energy of the fuel cell. In electrolyzer, according to the received electrical power, produced H_2 and maximum generation capacity can be calculated using Eqs. (37) and (38) respectively. The cost of HSS operation, is a function of its usage, which is expressed via Eq. (39).

$$0 \le \mathrm{H}_{2}{}^{hss}_{ch,t,\omega} \le \frac{\mathrm{H}_{2}{}^{hss}_{max}}{\eta^{hss}_{ch}} \quad \forall t,\omega \tag{27}$$

$$0 \le \mathrm{H}_{2}{}^{hss}_{dch,t,\omega} \le \mathrm{H}_{2}{}^{hss}_{max} \cdot \eta^{hss}_{dch} \quad \forall t,\omega \tag{28}$$

$$SoC^{hss}_{t,\omega} = SoC^{hss}_{t-1,\omega} + (\mathrm{H}_{2}{}^{hss}_{ch,t,\omega} \cdot \eta^{hss}_{ch} - \frac{\mathrm{H}_{2}{}^{hss}_{dch,t,\omega}}{\eta^{hss}_{dch}}) \quad \forall t,\omega \tag{29}$$

$$SoC^{hss}_{min} \le SoC^{hss}_{t,\omega} \le SoC^{hss}_{max} \quad \forall t,\omega \tag{30}$$

$$SoC^{hss}_{t_0} = SoC^{hss}_{int} \tag{31}$$

$$SoC^{hss}_{t_f} = SoC^{hss}_{fin} \tag{32}$$

$$\mathrm{H}_{2}{}^{hss}_{t,\omega} = \mathrm{H}_{2}{}^{hss}_{ch,t,\omega} - \mathrm{H}_{2}{}^{hss}_{dch,t,\omega} \quad \forall t,\omega \tag{33}$$

$$\mathrm{H}_{2}{}^{fc}_{t,\omega} = \frac{P^{fc}_{t,\omega}}{\eta^{fc}} \cdot \eta^{\mathrm{H}_2} \quad \forall t,\omega \tag{34}$$

$$0 \le P^{fc}_{t,\omega} \le P^{fc}_{max} \quad \forall t,\omega \tag{35}$$

$$H^{fc}_{t,\omega} = \mathrm{H}_{2}{}^{fc}_{t,\omega} \frac{1-\eta^{fc}}{\eta^{\mathrm{H}_2}} \quad \forall t,\omega \tag{36}$$

$$\mathrm{H}_{2}{}^{el}_{t,\omega} = \frac{P^{el}_{t,\omega}}{\eta^{\mathrm{H}_2}} \cdot \eta^{el} \quad \forall t,\omega \tag{37}$$

$$0 \le P^{el}_{t,\omega} \le P^{el}_{max} \quad \forall t,\omega \tag{38}$$

$$Cost^{hss}_{t,\omega} = \mathcal{A}^{hss} \cdot [\mathrm{H}_{2}{}^{hss}_{ch,t,\omega} + \mathrm{H}_{2}{}^{hss}_{dch,t,\omega}] \quad \forall t,\omega \tag{39}$$

where, $\mathrm{H}_{2}{}^{hss}_{ch,t,\omega}$, $\mathrm{H}_{2}{}^{hss}_{dch,t,\omega}$, $\mathrm{H}_{2}{}^{hss}_{t,\omega}$ and $SoC^{hss}_{t,\omega}$ represent charging, discharging and net H_2 power and state of charge for the hydrogen tank at time t and scenario ω, respectively. SoC^{HSS}_{max}, SoC^{HSS}_{min}, SoC^{EV}_{init} and SoC^{EV}_{fin} are respective parameters for maximum, minimum, initial and final energy levels of the HSS. η^{hss}_{ch}, η^{HSS}_{dch}, η^{fc}, η^{el} and η^{H_2} indicate efficiencies of charging and discharging of HSS, efficiencies of fuel cell and electrolyzer and conversion coefficient of hydrogen to power, accordingly. Moreover, $H^{fc}_{t,\omega}$, $P^{fc}_{t,\omega}$ and $P^{el}_{t,\omega}$ stand for produced thermal and electrical power of the fuel cell and electrical power consumption of the electrolyzer. Furthermore, $\mathrm{H}_{2}{}^{fc}_{t,\omega}$ and $\mathrm{H}_{2}{}^{el}_{t,\omega}$ indicate generated and consumed hydrogen by fuel cell and electrolyzer, respectively. Similarly, maximum H_2 capacity of the HSS, maximum allowable power of the fuel cell and electrolyzer are shown by $\mathrm{H}_{2}{}^{hss}_{m}ax$, $P^{fc}_{m}ax$ and $P^{el}_{m}ax$. Finally, $\mathcal{A}$, is the cost coefficients of using hydrogen tank.

2.5. Demand response

Aggregated demand response can be utilized as a VESS tool due to the similar charging/discharging behavior with ESS and intelligently managing the demand level. In fact, the VESS system could be implemented by existing network assets such as domestic refrigerators and freezers, and industrial heating loads. In this section, modeling for both electrical and thermal demands as flexible loads is presented. Further, the constraints related to the electrical responsive demand is expressed via Eqs. (40)–(43), while similar relations for thermal demands are shown in Eqs. (44)–(47). Revenue for executing demand response programs is shown via Eq. (48), which is obtained by the VESS operator.

$$P^{L,drp}_{t,\omega} = P^{L}_{t,\omega} + P^{L,up}_{t,\omega} - P^{L,down}_{t,\omega} \quad \forall t,\omega \tag{40}$$

$$0 \le P^{L,up}_{t,\omega} \le P^{L}_{t,\omega} \quad \forall t,\omega \tag{41}$$

$$0 \le P^{L,down}_{t,\omega} \le P^{L}_{t,\omega} \quad \forall t,\omega \tag{42}$$

$$\sum_{t=1}^{t_{fin}} P^{L,down}_{t,\omega} = \sum_{t=1}^{t_{fin}} P^{L,up}_{t,\omega} \quad \forall \omega \tag{43}$$

$$H^{L,drp}_{t,\omega} = H^{L}_{t,\omega} + H^{L,up}_{t,\omega} - H^{L,down}_{t,\omega} \quad \forall t,\omega \tag{44}$$

$$0 \le H^{L,up}_{t,\omega} \le H^{L}_{t,\omega} \quad \forall t,\omega \tag{45}$$

$$0 \le H^{L,down}_{t,\omega} \le H^{L}_{t,\omega} \quad \forall t,\omega \tag{46}$$

$$\sum_{t=1}^{t_{fin}} H^{L,down}_{t,\omega} = \sum_{t=1}^{t_{fin}} H^{L,up}_{t,\omega} \quad \forall \omega \tag{47}$$

$$Rev^{dr}_{\omega} = \mathcal{A}^{dr} \cdot [\sum_{t=1}^{t_{fin}} P^{L,down}_{t,\omega} + \sum_{t=1}^{t_{fin}} H^{L,down}_{t,\omega}] \quad \forall \omega \tag{48}$$

where $P^{L,drp}_{t,\omega}$, $P^{L}_{t,\omega}$, $P^{L,up}_{t,\omega}$ and $P^{L,down}_{t,\omega}$, are respective symbols for electrical demand after participating in demand response, basic demand, connected power and curtailed power in demand response process. Besides, $H^{L,drp}_{t,\omega}$, $H^{L}_{t,\omega}$, $H^{L,up}_{t,\omega}$ and $H^{L,down}_{t,\omega}$, stand for thermal demand after participating in demand response, basic demand, connected and curtailed thermal demand.

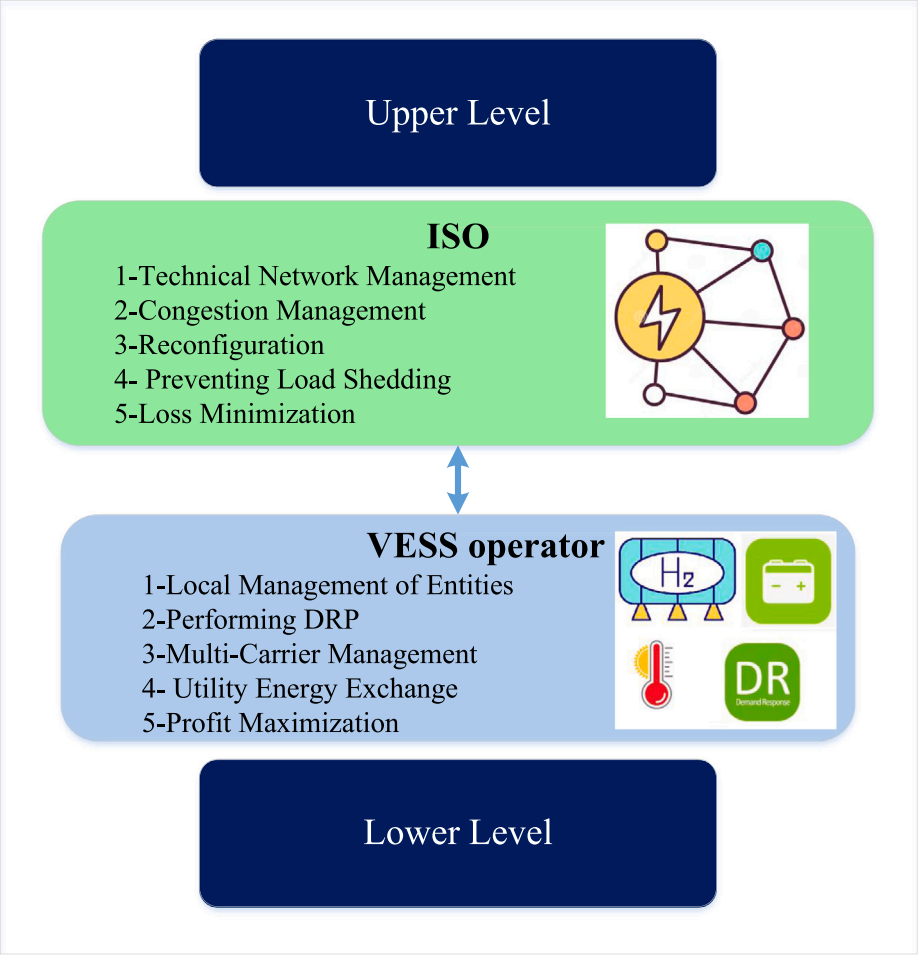

Fig. 2. Proposed Bi-Level Congestion Management Approach.

2.6. Energy balance constraints

In any carrier of energy, a balance between generation and consumption should be maintained at every hour. Eqs. (49)–(51) show the constraints for energy balance in electrical, thermal and hydrogen carriers, accordingly.

$$P^{utility}_{t,\omega} + \sum_{fc} P^{fc}_{t,\omega} = \sum_{b} P^{b}_{t,\omega} + \sum_{EV} P^{EV}_{t,\omega} + \sum_{p2ht} P^{p2ht}_{t,\omega} + \sum_{el} P^{el}_{t,\omega} + \sum_{L,ndrp} P^{L}_{t,\omega} + \sum_{L,drp} P^{L,drp}_{t,\omega} \quad \forall t,\omega \tag{49}$$

$$H^{utility}_{t,\omega} + \sum_{fc} H^{fc}_{t,\omega} + \sum_{p2ht} H^{p2ht}_{t,\omega} = \sum_{tes} H^{tes}_{t,\omega} + \sum_{L,ndrp} H^{L}_{t,\omega} + \sum_{L,drp} H^{L,drp}_{t,\omega} \quad \forall t,\omega \tag{50}$$

$$\mathrm{H}_{2}{}^{utility}_{t,\omega} + \sum_{el} H^{el}_{t,\omega} = \sum_{hss} \mathrm{H}_{2}{}^{hss}_{t,\omega} + \sum_{fc} H^{fc}_{t,\omega} + \sum_{L} H^{L}_{t,\omega} \quad \forall t,\omega \tag{51}$$

2.7. Power flow

The distribution network consists of various ESSs aggregated as a VESS, and the ISO should determine the optimum power transaction of each entity and the exchanged power with the utility grid considering the network constraints. Further, distribution networks are operated usually in radial forms and it is assumed that the first bus is connected to the utility grid and has a flexible power injection with a voltage of 1 *p.u*. The following equations show the linearized convex power flow in such networks, which have been utilized in distribution networks considerably [29,30]. In addition, reconfiguration is a tool for the system operator to handle congestion and contingencies. A binary variable $\gamma_{i,k}$ is defined as 1 when there is a connection between buses i and k. Further, big M approach is utilized to model a linear form. In this case, if $\gamma_{i,k}$ becomes 1, Eqs. (54) and (55), Eqs. (56) and (57), and Eqs. (58) and (59), become equality constraints. i, j and k are indices for the bus number. r_{ik}, x_{ik}, P_{ik} and Q_{ik} are representatives for resistance, reactance, passing active and reactive power of line ik, respectively. Consequently, U_k shows the voltage magnitude of the bus #k. $\mathfrak{T}$ is the set of buses connected to a specific bus and are ahead of that in the radial formation.

$$P^{net}_{k,t} = P^{b}_{k,t} + P^{L}_{k,t} + P^{L,drp}_{k,t} - P^{fc}_{k,t} + P^{el}_{k,t} - P^{L,shedded}_{k,t} \tag{52}$$

$$Q^{net}_{k,t} = Q^{L}_{k,t} + Q^{L,drp}_{k,t} - Q^{L,shedded}_{k,t} \tag{53}$$

$$P^{net}_{k,t} \geq P_{ik,t} - \sum_{j\in\mathfrak{T}} P_{kj,t} - [1-\gamma_{ik,t}]\cdot M \tag{54}$$

$$P^{net}_{k,t} \leq P_{ik,t} - \sum_{j\in\mathfrak{T}} P_{kj,t} + [1-\gamma_{ik,t}]\cdot M \tag{55}$$

$$Q^{net}_{k,t} \geq Q_{ik,t} - \sum_{j\in\mathfrak{T}} Q_{kj,t} - [1-\gamma_{ik,t}]\cdot M \tag{56}$$

$$Q^{net}_{k,t} \leq Q_{ik,t} - \sum_{j\in\mathfrak{T}} Q_{kj,t} + [1-\gamma_{ik,t}]\cdot M \tag{57}$$

$$U_{k,t} \geq U_{i,t} - (r_{ik}P_{ik,t} + x_{ik}Q_{ik,t})/U_{1,t} - [1-\gamma_{ik,t}]\cdot M \tag{58}$$

$$U_{k,t} \leq U_{i,t} - (r_{ik}P_{ik,t} + x_{ik}Q_{ik,t})/U_{1,t} + [1-\gamma_{ik,t}]\cdot M \tag{59}$$

$$U^{min}_{i} \leq U_{i,t} \leq U^{max}_{i} \tag{60}$$

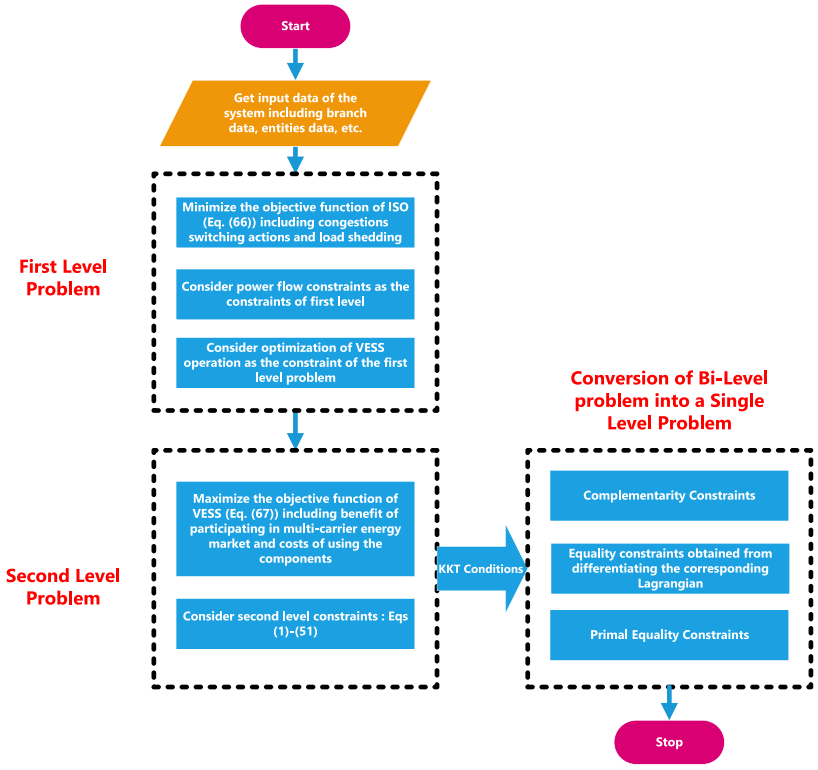

Fig. 3. Flowchart of the procedure.

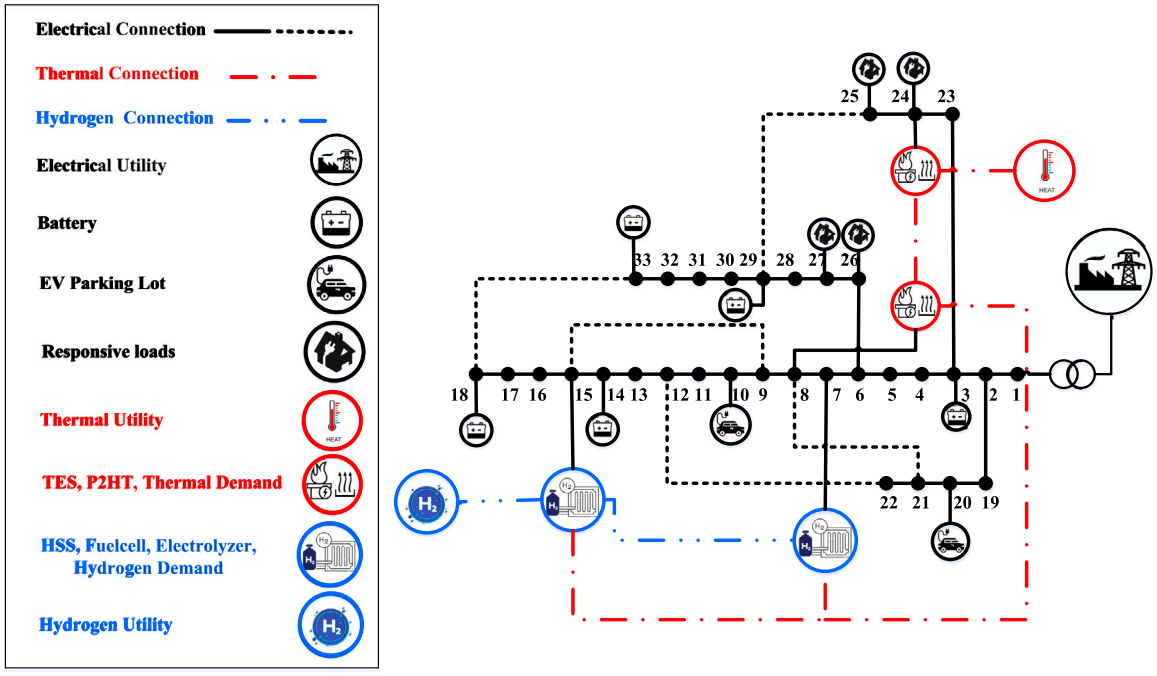

Fig. 4. IEEE 33-bus test system in the presence of VESS entities and various energy carriers.

$$-\gamma_{ik,t} \cdot P_{ik}^{max} \le P_{ik,t} \le \gamma_{ik,t} \cdot P_{ik}^{max} \tag{61}$$

$$-\gamma_{ik,t} \cdot Q_{ik}^{max} \le Q_{ik,t} \le \gamma_{ik,t} \cdot Q_{ik}^{max} \tag{62}$$

Also for radial operation, the spanning tree approach is selected, which can be shown by [31]:

$$\beta_{ik,t} + \beta_{ki,t} = \gamma_{ik,t} \tag{63}$$

$$\sum_{k} \beta_{k0,t} = 0 \tag{64}$$

$$\sum_{k} \beta_{ki,t} \le 1 \tag{65}$$

In this approach, every node in the network has one parent node and the first bus has no parent. Eq. (63) demonstrates that if ith node is the parent of the jth node or vice versa, then there is a link between them,

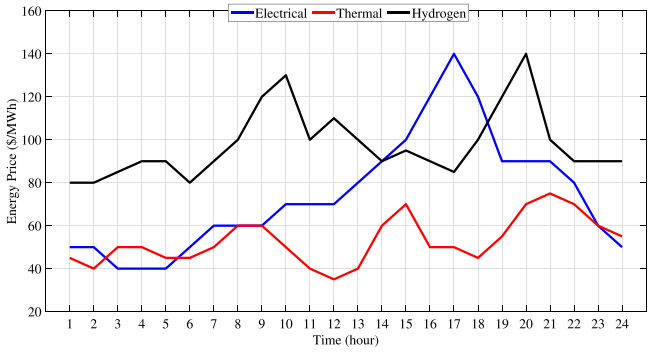

Fig. 5. Mean energy exchange price during the scheduling period.

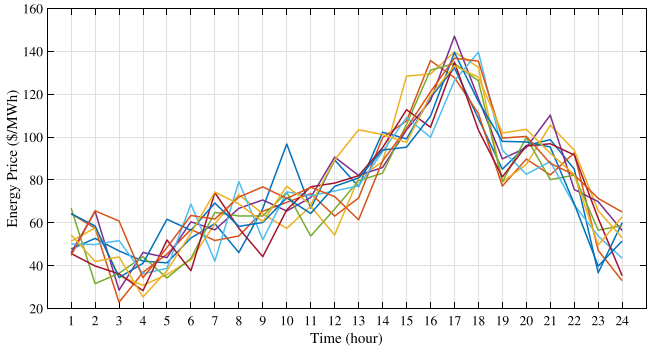

Fig. 6. 10 different scenarios for electrical energy exchange price during the scheduling period.

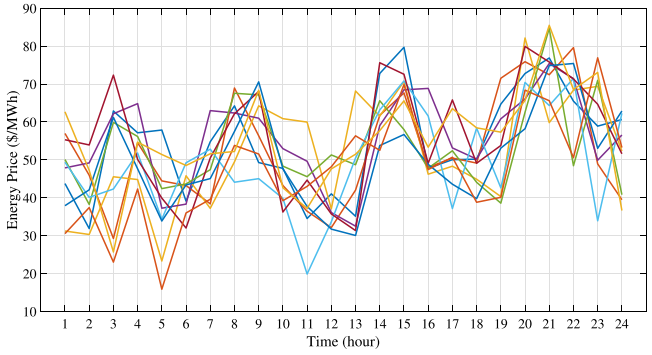

Fig. 7. 10 different scenarios for thermal energy exchange price during the scheduling period.

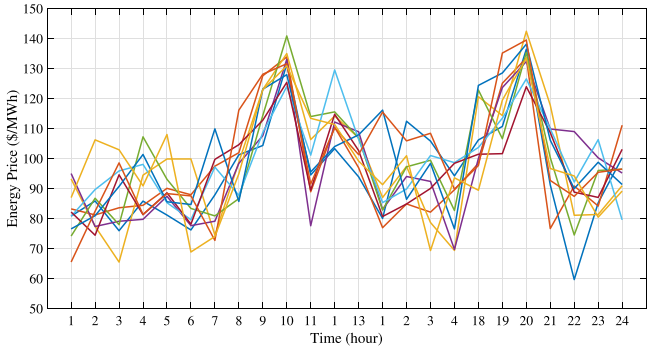

Fig. 8. 10 different scenarios for hydrogen energy exchange price during the scheduling period.

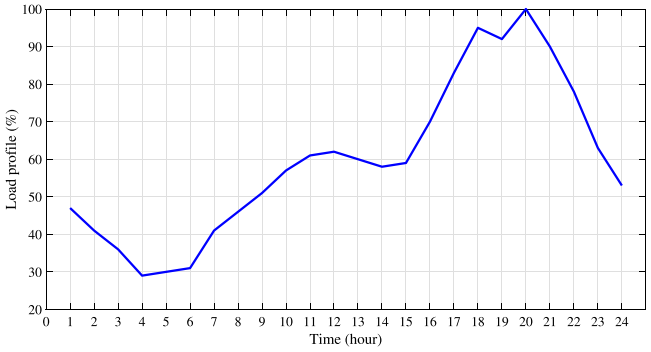

Fig. 9. Load profile percentage.

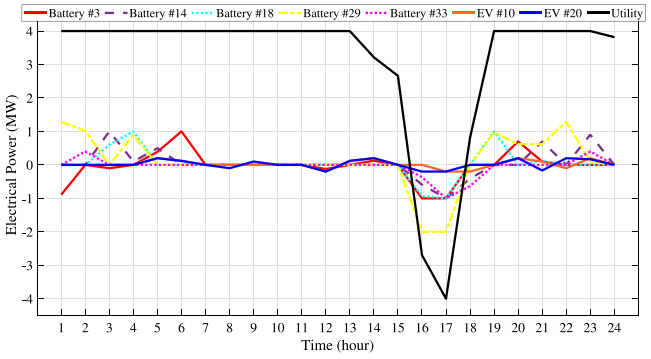

Fig. 10. Optimal electric output power of the batteries, EVs and utility grid transactions in ***CS1***.

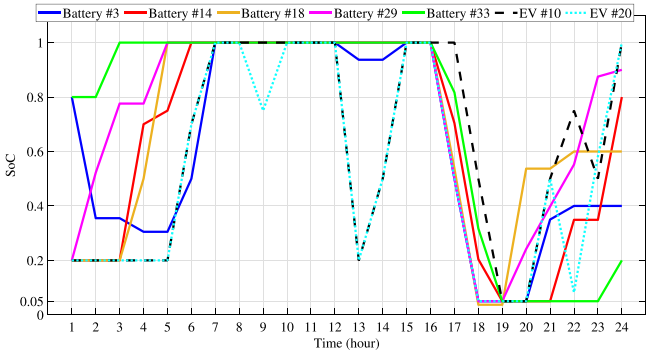

Fig. 11. SoC of the batteries and EVs in ***CS1***.

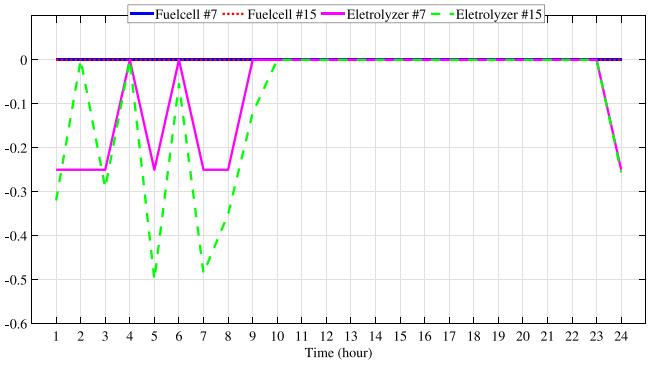

Fig. 12. Optimal electric power generation/consumption of the fuel cells and electrolyzer units in ***CS1***.

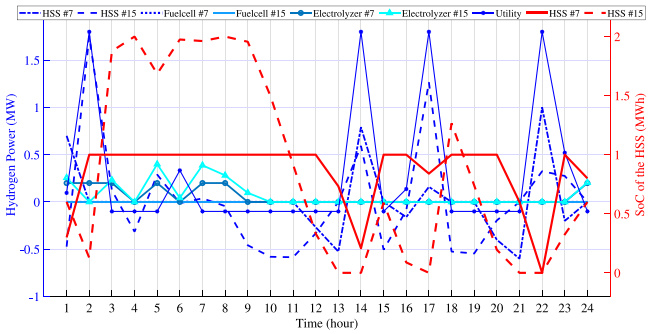

Fig. 13. Optimal hydrogen power generation/consumption of the fuel cells, electrolyzers, HSS units, utility transactions and energy level of the HSSs in ***CS1***.

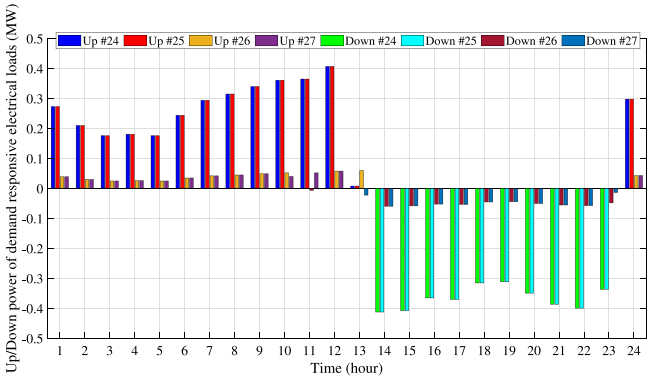

Fig. 14. Demand response results of the electric demands in ***CS1***.

which is shown by binary variable γ_{ik}. To avoid multiple parents for the first bus, Eq. (64) is applied and finally Eq. (65) stands for forcing each bus to have one parent bus.

2.8. Uncertainty modeling

In this study, scenario-based approach is utilized for modeling of energy prices as uncertainty sources in the problem. In fact, Monte-Carlo simulation would be used for generating different scenarios as it is widely used and the most suitable approach for stochastic problems [32]. Further, the number of generated scenarios should be high in order to obtain accurate answer for the problem, however, in this regard, the computational burden and solution time are significantly increased. Accordingly, an appropriate scenario reduction approach should be applied to reduce the number of scenarios to facilitate the solution process. In other words, scenario reduction approach tries to shrink a set of scenarios while applying the same amount of stochastic data intact. In this study, fast backward selection algorithm is used for scenario reduction based on probability distance [33]. For this goal, *"SCENRED"* tool provided by GAMS software is utilized.

2.9. Bi-level modeling of the problem

In this subsection, the objective function of the proposed method for congestion management is presented. Congestion management is maintaining voltages and power passing within predefined limits in contingency or emergency situations. In this study, congestion management is controlled by the ISO with network reconfiguration in the presence of VESS in the system. The problem is formulated as a bi-level optimization with ISO in the upper, which is responsible for network operational costs, technical constraints and congestion management, while the VESS operator in the lower level trying to obtain the maximum benefit. Accordingly, Fig. 2 shows upper and lower levels in the optimization process.

In this subsection, the formulation of the optimization problem in the upper and lower levels is presented. The objective function of the ISO as performer of the upper level, along with its constraints, is as follows:

$$\min \sum_{t} \left\{ \sum_{NO} \gamma_{ik,t} \cdot C_{sw} + \sum_{NC} (1-\gamma_{ik,t}) \cdot C_{sw} + \lambda^{sh} \cdot \sum_{k} P_{k,t}^{L,sh} + \lambda^{cm} \cdot \sum_{ik} \frac{P_{ik,t}}{P_{ik}^{r}} \right\} \tag{66}$$

subject to: Eqs. (52)–(65) $\forall t$

The objective function is composed of three main terms trying to minimize switching actions and avoid load shedding and minimizing the proportion of the passage power to the rated power of the lines to manage the congestion. Also, ISO performs a power flow in the reconfigurable network using Eqs. (52) to (65) maintaining the voltage and current limits in a predefined interval. C_{sw} and λ^{sh} are the price of switching actions and load shedding and $P_{k,t}^{L,sh}$ is the amount of curtailed load at bus #k at time t. Subsequently, P_{ik}^{r} is the rated power of the line ik. However, some variables are dependant to VESS schedules and can be obtained from the lower level problem including $P_{k,t}^{b}$, $P_{k,t}^{L,drp}$, $P_{k,t}^{L,shedded}$, $P_{k,t}^{p2ht}$, $P_{k,t}^{fc}$ and $P_{k,t}^{el}$. These variables are the battery power, flexible loads, shedded power, P2HT unit power, fuel cell and electrolyzer power, respectively. In the lower level, the VESS maximizes its benefit, which is shown in terms of below optimization process:

$$\begin{aligned} &P_{k,t}^{b}, P_{k,t}^{L,drp}, P_{k,t}^{L,shedded}, P_{k,t}^{fc}, P_{k,t}^{el} \quad \forall k,t \in arg \left\{ max \sum_{t} \sum_{\omega} \pi_{\omega} \times \right. \\ &\left[\lambda_{t,\omega}^{elec} \cdot \sum_{L} (P_{t}^{L} - P_{t}^{L,shedded}) + \lambda_{t,\omega}^{therm} \cdot \sum_{L} H_{t}^{L} + \lambda_{t}^{H_2} \cdot \sum_{L} \mathrm{H}_{2_t}{}^{L} - \right. \\ &\sum_{b} Cost_{t,\omega}^{b} - \sum_{EV} Cost_{t,\omega}^{EV} - \sum_{tes} Cost_{t,\omega}^{tes} - \sum_{hss} Cost_{t,\omega}^{hss} + Rev_{\omega}^{dr} - \\ &\left. \left. \lambda_{t,\omega}^{elec} \cdot P_{t,\omega}^{utility} - \lambda_{t,\omega}^{therm} \cdot H_{t,\omega}^{utility} - \lambda_{t,\omega}^{\mathrm{H}_2} \cdot \mathrm{H}_{2_{t,\omega}}{}^{utility} \right] \right\} \\ &\text{subject to: Eqs. (1)–(51)} \quad \forall t, \omega \end{aligned} \tag{67}$$

In above formulations, ω is the scenario counter for energy price and π_{ω} is its weight. The VESS operator tries to gain benefit by selling energy to the utility and loads in higher price periods and storing the energy in lower price hours.

To enable the ISO to implement this approach in a real network, some infrastructure are required. The networks with switching capabilities and fast and secure communication infrastructure, which provide easy access to price data and market clearing procedures, are compatible with this approach. Also, infrastructures for thermal and hydrogen energy carriers besides the electrical network would be required.

3. Solution methodology

A general bi-level optimization problem consists of two levels with distinct objective functions and limitations. Thus,it is challenging to select solver for these types of problems, and achieved by converting them into a single level problem by mathematical program with equilibrium constraints (MPEC) [34]. However, this method is applicable only if the lower level problem is convex, and consequently substituted with its Karush–Kuhn Tucker (KKT) condition. All the constraints and formulation of the lower level problem is linear and convex and consequently MPEC could be applied. In addition, the KKT conditions of optimization problem can be presented in following equations:

$$\mathcal{L}(x,\mu,\lambda) = f(x) + \lambda^{T} h(x) + \mu^{T} g(x) \tag{68}$$

$$\nabla_{x} \mathcal{L}(\bar{x},\mu,\lambda) = 0 \tag{69}$$

$$\nabla_{\lambda} \mathcal{L}(\bar{x},\mu,\lambda) = 0 \tag{70}$$

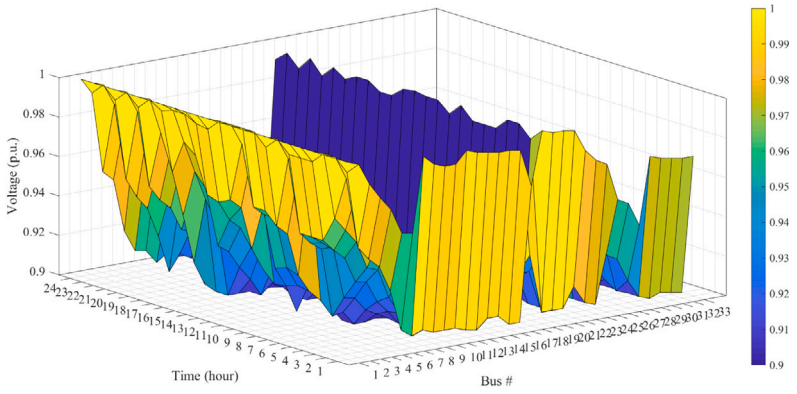

Fig. 15. Voltage of different buses in ***CS1***.

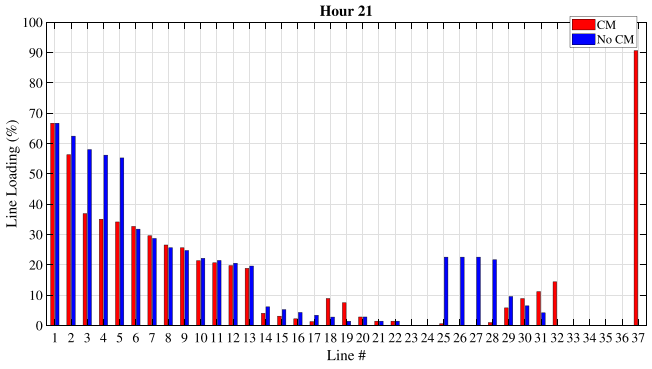

Fig. 16. Line loadings without/with congestion management (CM) at hour 21 in ***CS1***.

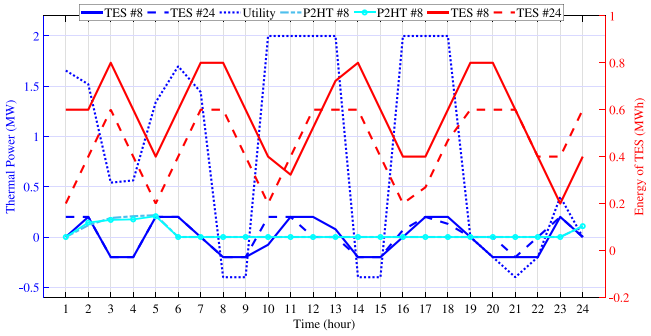

Fig. 19. Optimal thermal power of the P2HT, TES units, utility transactions and energy level of the TESs in ***CS2***.

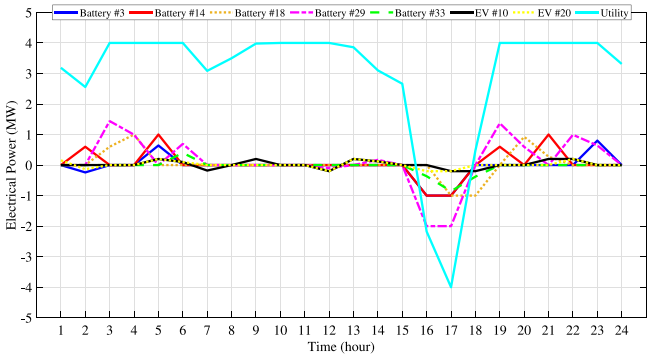

Fig. 17. Optimal electric output power of the batteries, EVs and utility grid transactions in ***CS2***.

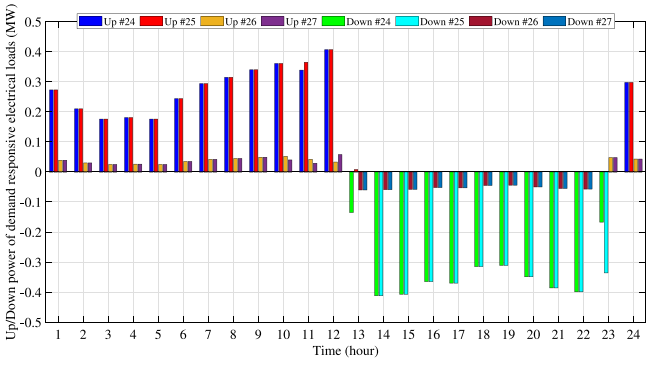

Fig. 20. Demand response results of the electric demands in ***CS2***.

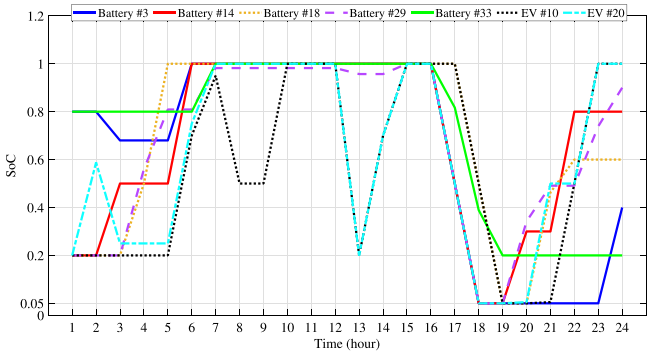

Fig. 18. SoC of the batteries and EVs in ***CS2***.

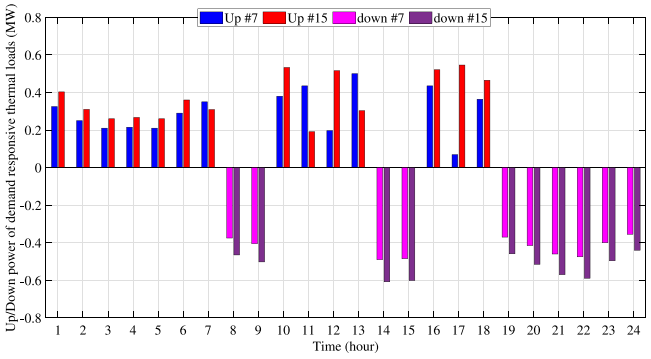

Fig. 21. Demand response results of the thermal demands in ***CS2***.

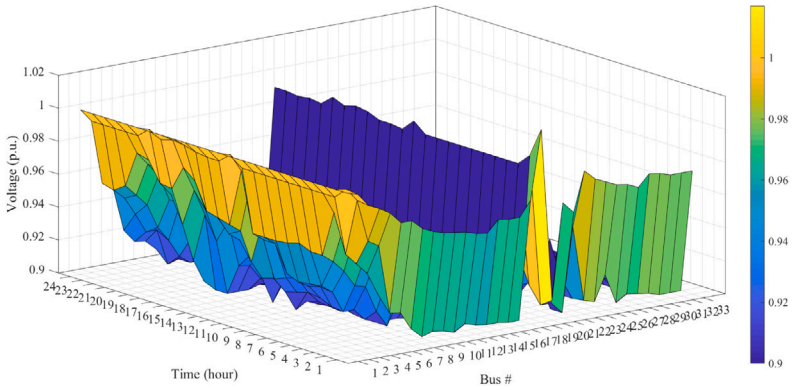

Fig. 22. Voltage of different buses in ***CS2***.

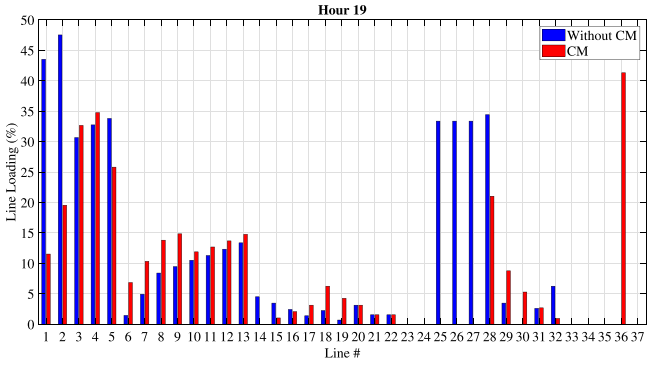

Fig. 23. Line loadings without/with congestion management (CM) at hour 19 in ***CS2***.

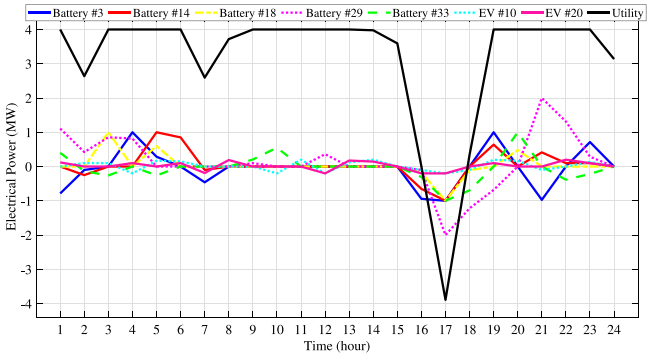

Fig. 24. Optimal electric output power of the batteries, EVs and utility grid transactions in ***CS3***.

$$\nabla_{\mu}\mathcal{L}(\bar{x},\mu,\lambda) \leq 0 \tag{71}$$

$$\mu^{T}\nabla_{\mu}\mathcal{L}(\bar{x},\mu,\lambda) = 0 \tag{72}$$

$$\mu \geq 0 \tag{73}$$

The equivalent of Eq. (72) is $\mu_j \cdot g_j(\bar{x}) = 0$ due to Eqs. (71) and (73). This can bring non-linearity to the problem modeling and it should be linearized, which can be obtained by employing an auxiliary binary

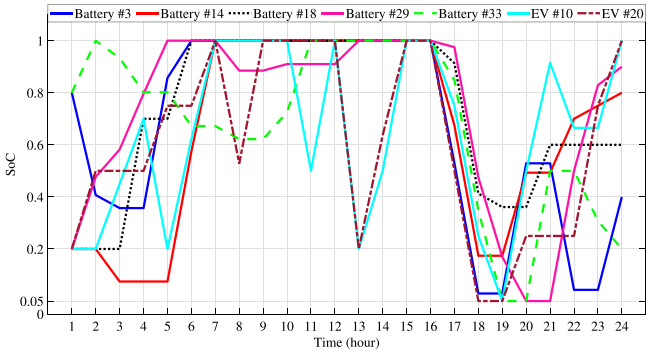

Fig. 25. SoC of the batteries and EVs in ***CS3***.

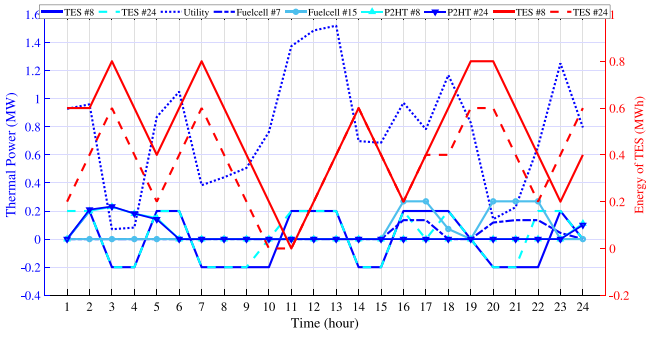

Fig. 26. Optimal thermal power of the fuel cells, P2HT, TES units, utility transactions and energy level of the TESs in ***CS3***.

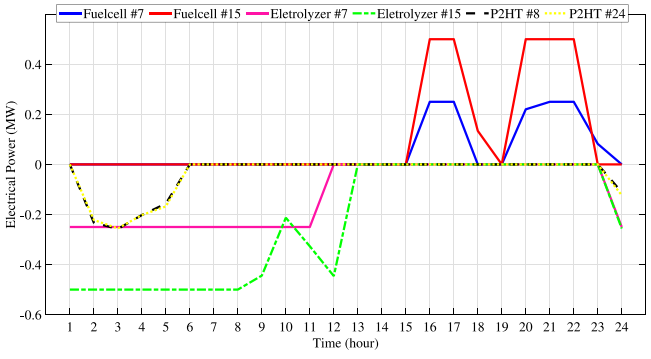

Fig. 27. Optimal electric power generation/consumption of the fuel cells, electrolyzers and P2HT units in ***CS3***.

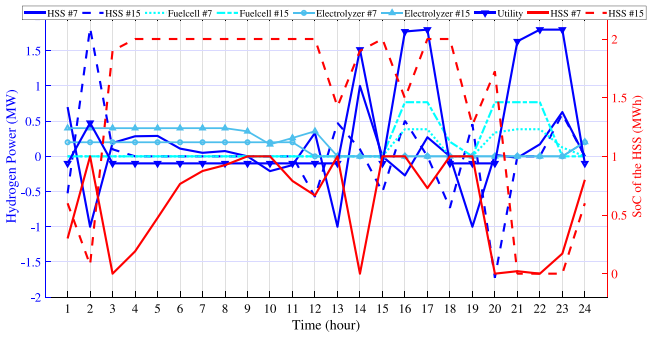

Fig. 28. Optimal hydrogen power generation/consumption of the fuel cells, electrolyzers, HSS units, utility transactions and energy level of the HSSs in ***CS3***.

variable (ζ) and big M as follows:

$$g_j(\bar{x}) \leq \zeta \cdot M \tag{74}$$

$$\mu_j \leq (1-\zeta) \cdot M \tag{75}$$

Using the KKT conditions and the linearity of the original problem, the bilevel model can be converted into a single level, and MIP model, which could be solved by commercial software. Fig. 3 shows the flowchart of solution procedure.

4. Simulation results

In this section, simulations on IEEE 33-bus test system are presented to evaluate the effectiveness of the proposed methodology. The problem is solved using GAMS software and CPLEX solver on a system with Core i7 CPU and 8 GB of RAM. Fig. 4 shows the locations of the VESS in IEEE 33-bus distribution system. The VESS is integrated with batteries, EVs, thermal energy storage systems, hydrogen storage systems alongside with fuel cells and electrolyzers. In this regard, electrical, thermal and hydrogen carriers are interwoven and operated simultaneously. Flexible loads are included at buses #24, #25, #26 and #27 as assistants of VESS operator. Also thermal demands participate in demand response. The characteristics of the units are shown in Tables 2 to 5. The parking lots provide space for EVs parking while charging and it is assumed that EVs arrival times to be in hours 01:00 and 13:00 while the full charge will occur at 12:00 and 24:00. The switching cost in reconfiguration is assumed to be 4$ per switching. Mean energy exchange price during the scheduling period is shown in Fig. 5. In the simulation process, 1000 scenarios are generated by Monte-Carlo simulation and using *"SCENRED"* tool provided by GAMS software, the total number of scenarios has been reduced to the final 20 scenarios. Figs. 6, 7 and 8 show ten sample scenarios for energy exchange price for each carrier of energy. Moreover, load profile percentage at each hour for the test system is shown in Fig. 9. The demand level for each bus is the basic demand in the IEEE 33-bus test system which is multiplied by the load profile percentage for various hours of the scheduling period. The voltage variations are allowed between 0.9 and 1.1 *p.u* and the voltage of the first bus is 1 *p.u*. Four case studies (**CS**s) are considered as follows to study the effect of each type of energy storage system:

- *Case study 1 (**CS1**):* It is assumed that the VESS contains electrical and hydrogen storage systems and benefits from demand response programs. The thermal storage systems are not considered.
- *Case study 2 (**CS2**):* It is assumed that the VESS contains electrical and thermal storage systems and benefits from demand response programs, while ignoring the hydrogen storage systems.
- *Case study 3 (**CS3**):* It is assumed that the VESS contains all electrical, thermal and hydrogen storage systems but responsive loads are excluded.

Table 2
Characteristics of battery energy storage systems.

Bus #	Initial energy (MWh)	Final energy (MWh)	Capacity (MWh)	P_{max} (MW)	η^b_{ch}	η^b_{dch}
3	1.6	0.8	2	1	0.9	0.9
14	0.4	1.6	2	1	0.9	0.9
18	0.4	1.2	2	1	0.9	0.9
29	0.8	3.6	4	2	0.9	0.9
33	1.6	0.4	2	1	0.9	0.9

Table 3
Characteristics of EV parking lots.

Bus #	Initial energy (MWh)	Final energy (MWh)	Capacity (MWh)	P_{max} (MW)	η^{EV}_{ch}	η^{EV}_{dch}
10	0.08	0.4	0.4	0.2	0.9	0.9
20	0.08	0.4	0.4	0.2	0.9	0.9

- *Case study 4 (**CS4**):* It is assumed that the VESS benefits from all electrical, thermal and hydrogen storage systems and also demand response programs.

4.1. CS1

This case study assumes that the VESS contains electrical and hydrogen storage systems, and obtains benefits from demand response programs while ignoring the thermal units. In fact, the results of the optimization are depicted in Figs. 10–14. The total revenue obtained by the VESS is $2781 during 24 h. Figs. 10 and 11 show electrical power transactions of batteries, EVs and utility and the SoC of the electrical storages, respectively. Moreover, the charging occurs during the lower price periods and get discharged in the higher price periods. Between hours 15:00 to 18:00, all units are selling power to the utility grid which is shown by its curve. This is compatible with the mean price curve shown in Fig. 5. The SoCs of different entities are shown in Fig. 11. During high price times, the SoC decreases to its minimum allowable level, and increases to its maximum in lower price periods. EVs parking lots participate in energy management as VESS to get more revenue for the system. For instance, at 18:00 and 19:00, it is fully discharged to the minimum allowable level and try to satisfy the customers by fully charging them in the departure time.

In Fig. 12 electric generation/ consumption of fuel cell and electrolyzer units are depicted. When the electricity price is less than hydrogen price, electrolyzer utilizes electrical power to produce hydrogen, which occurs in early hours of the day. In periods with higher electricity prices, fuel cell consumes hydrogen to produce electrical power, and the curves for hydrogen carrier are shown in Fig. 13. In this figure, hydrogen generation/ consumption of different units are illustrated, and depicts the hydrogen transactions with utility. The HSS is charged via electrolyzer or utility in low price hours of hydrogen and gets discharged by fuel cell/utility during high price periods. In these figures, interconnectivity of hydrogen and electrical carriers are shown, and the interfacing units are fuel cells and electrolyzers. For instance, electrolyzers are consuming electrical energy at hour 7:00 to produce hydrogen due to higher price of hydrogen in comparison with electricity.

Demand response results for electrical demands are shown in Fig. 14. DRP is executed in the same manner as energy storage systems, where a demand reduction shows in higher price hours and increases the demand in lower prices hours, while gaining benefits for VESS. Comparing the demand response results with the SoC level, which shows a similar pattern and such as the lower/higher SoCs during higher/lower price periods, the demand level are reduced/increased in the flexible loads.

Figs. 15 and 16 show voltage of the buses and line loadings in % at 21:00. It is shown that voltage variations are limited between

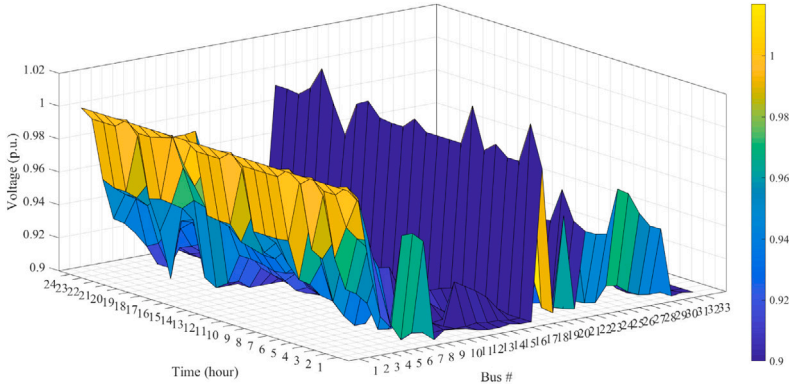

Fig. 29. Voltage of different buses in ***CS3***.

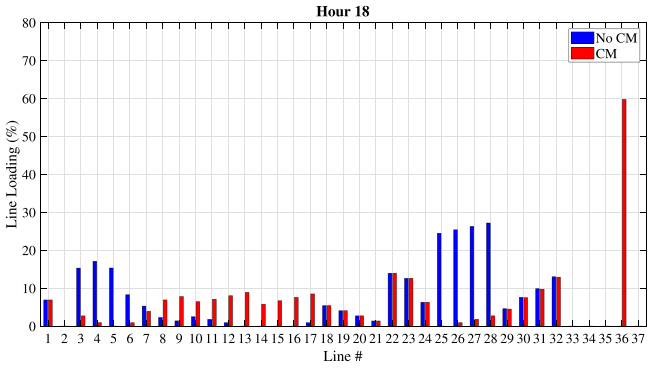

Fig. 30. Line loadings without/with congestion management (CM) at hour 18 in ***CS3***.

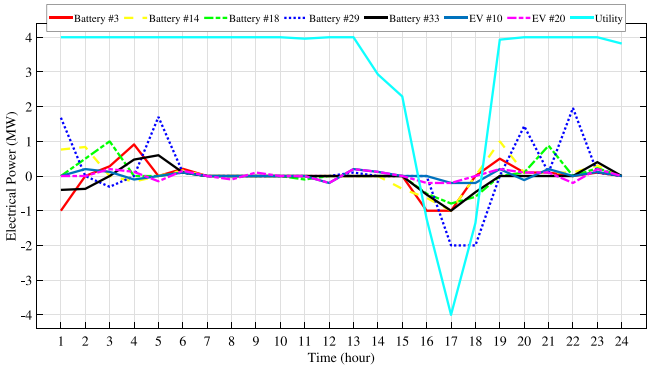

Fig. 31. Optimal output electric power of the batteries, EVs and utility grid transactions in ***CS4***.

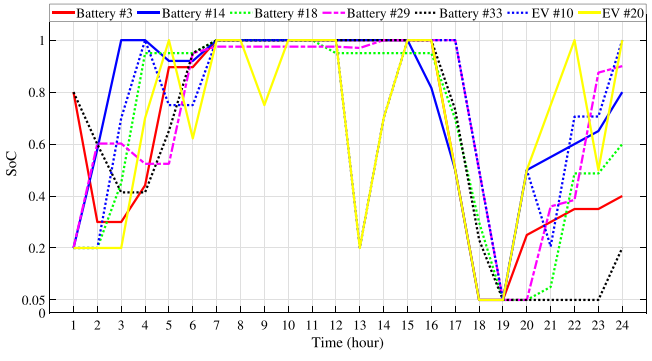

Fig. 32. SoC of the batteries and EVs in ***CS4***.

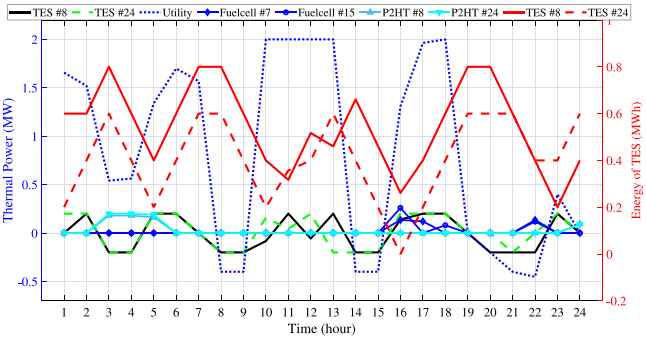

Fig. 33. Optimal thermal power of the fuel cells, P2HT, TES units, utility transactions and energy level of the TESs in ***CS4***.

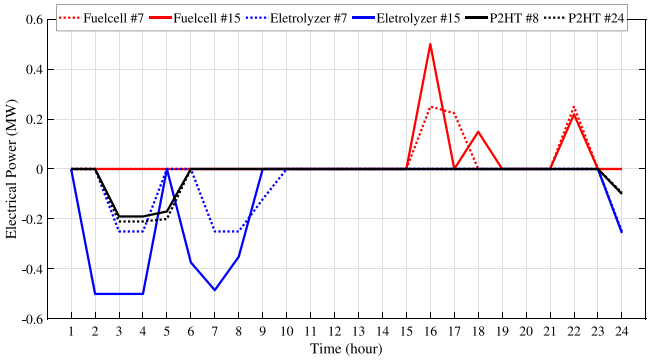

Fig. 34. Optimal electric power generation/consumption of the fuel cells, electrolyzers and P2HT units in ***CS4***.

1 p.u. and 0.9 p.u. The congestion management could be utilized to observe a drop in overall line loadings, and the switching results are shown in Table 6. The results are depicted in Fig. 15 which classified line loadings in two conditions: (i) system is capable of switching and congestion management. (ii) system lacks switching option and accordingly is incapable of performing congestion management. Using congestion management, the overall line loadings have been reduced.

4.2. CS2

This case study assumes that the VESS contains electrical and thermal storage systems and benefits from demand response programs, while ignoring the hydrogen units. In particular, the results of the optimization are depicted in Figs. 17–21. The total revenue obtained by the VESS is $892 during 24 h. In comparison with the previous

Table 4
Characteristics of TESs.

Bus #	Initial energy (MWh)	Final energy (MWh)	Capacity (MWh)	H^{tes}_{max} (MW)	H^{p2ht}_{max} (MW)	η^{tes}_{loss}	η^{tes}_{ch}	η^{tes}_{dch}	η^{p2ht}
8	0.6	0.4	0.8	0.2	0.2	0.05	0.95	0.95	0.95
24	0.2	0.6	0.6	0.2	0.2	0.05	0.95	0.95	0.95

Table 5
Characteristics of HSSs.

Bus #	Initial energy (MWh)	Final energy (MWh)	Capacity (MWh)	H_{2max}^{hss} (MW)	P^{fc}_{max} (MW)	P^{el}_{max} (MW)	η^{hss}_{ch}	η^{hss}_{dch}	η^{fc}	η^{el}
7	0.6	0.6	2	0.5	0.5	0.5	0.95	0.95	0.65	0.8
15	0.6	0.6	1	0.5	0.25	0.25	0.95	0.95	0.65	0.8

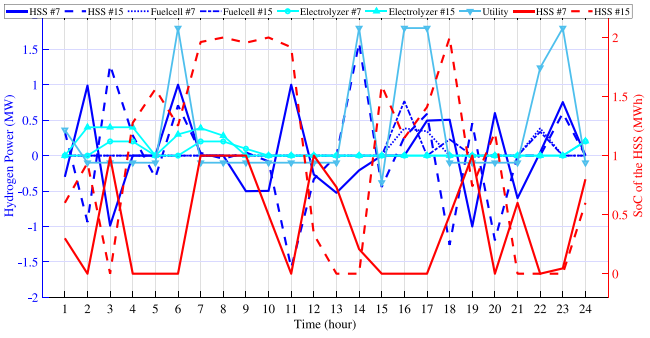

Fig. 35. Optimal hydrogen power generation/consumption of the fuel cells, electrolyzers, HSS units, utility transactions and energy level of the HSSs in ***CS4***.

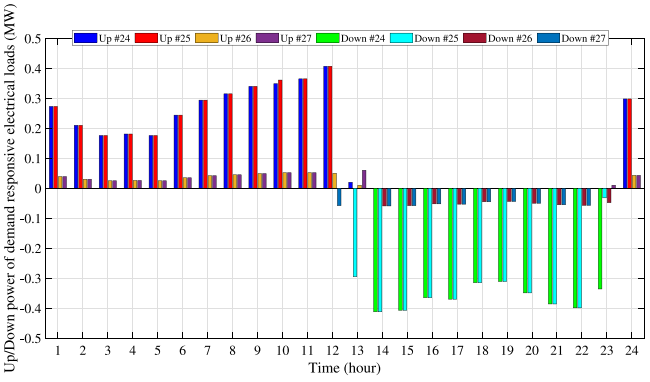

Fig. 36. Demand response results of the electric demands in ***CS4***.

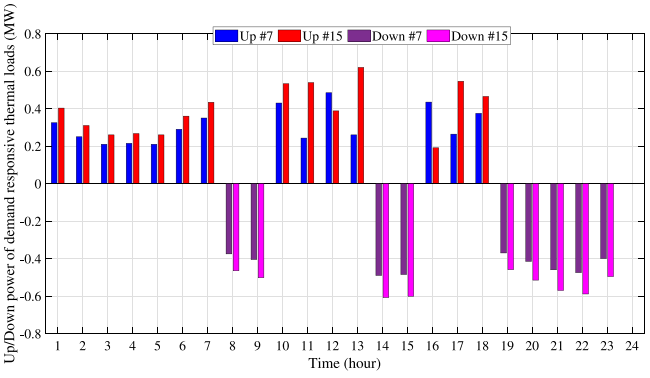

Fig. 37. Demand response results of the thermal demands in ***CS4***.

case study, it shows a significant reduction in the VESS revenue, which shows the effect of participating in the hydrogen market and

Table 6
Optimal switching of the ISO in ***CS1***.

Time	Open switches	Time	Open switches
1	12-22, 9-15, 8-21, 18-33, 25-29	13	12-22, 9-15, 8-21, 18-33, 25-29
2	12-22, 9-15, 8-21, 25-29,31-32	14	12-22, 9-15, 8-21, 18-33, 25-29
3	12-22, 9-15, 8-21, 25-29,31-32	15	12-22, 9-15, 8-21, 18-33, 25-29
4	12-22, 9-15, 8-21, 25-29,31-32	16	12-22, 9-15, 8-21, 18-33, 25-29
5	12-22, 9-15, 8-21, 18-33, 25-29	17	12-22, 9-15, 8-21, 18-33, 25-29
6	12-22, 9-15, 8-21, 18-33, 25-29	18	12-22, 9-15, 8-21, 18-33, 25-29
7	12-22, 9-15, 8-21, 18-33, 25-29	19	12-22, 9-15, 8-21, 18-33, 25-29
8	12-22, 9-15, 8-21, 25-29,31-32	20	12-22, 9-15, 8-21, 18-33, 25-29
9	12-22, 9-15, 8-21, 18-33, 25-29	21	12-22, 9-15, 8-21,24-25,26-27
10	12-22, 9-15, 8-21, 18-33, 25-29	22	12-22, 9-15, 8-21,24-25,26-27
11	12-22, 9-15, 8-21, 18-33, 25-29	23	12-22, 9-15, 8-21, 18-33, 25-29
12	12-22, 9-15, 15-16,8-21, 25-29	24	12-22, 9-15, 8-21, 18-33, 25-29

utilizing hydrogen storage systems. In Figs. 17 and 18 electrical power transactions of batteries, EVs and utility and the SoC of the electrical storages are demonstrated. As discussed earlier, the charging occurs in lower price hours, while the discharging occurs in higher price hours. Between hours 15:00 to 17:00, the power is sold to the utility grid because of the mean price curve shown in Fig. 5. The SoCs of different entities are shown in Fig. 18 and again during high price times, the SoC decreases to its minimum allowable level and increases to its maximum in lower price periods.

Fig. 19 presents the optimal scheduling of the thermal units, i.e. P2HT and TES units with utility transactions besides the energy level of the TESs. According to the figure, the TES systems harvest energy in low price hours and inject the thermal energy to the grid in high price hours. Moreover, P2HT units are operated in hours with the dominance of thermal energy price over the electricity price such as late hours of the night and early hours of the morning.

Figs. 20 and 21 shows the thermal and electrical power displacements due to demand response programs. Comparing the demand response results with the SoC level of the both thermal and electrical storage which shows a similar pattern such as the lower/higher SoCs during higher/lower price periods, the demand level are reduced/increased in the flexible loads.

Figs. 22 and 23 stand for voltage magnitude of the buses and line loadings at hour 19:00, and the result shows a reduction in line loading. Further, the switching results are shown in Table 7.

4.3. CS3

In this case study, it is assumed that the VESS contains electrical, thermal and hydrogen storage systems and excludes responsive loads. The results of the optimization are depicted in Figs. 24–28. In this case study, the total revenue achieved by the VESS owner during 24-hour period is $2927. In Figs. 24 and 25 electrical power transactions of batteries, EVs and utility and the SoC of the electrical storage units are shown, respectively.

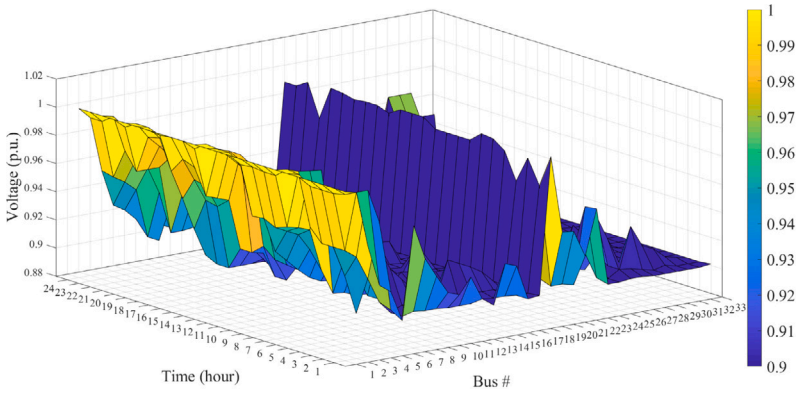

Fig. 38. Voltage of different buses in ***CS4***.

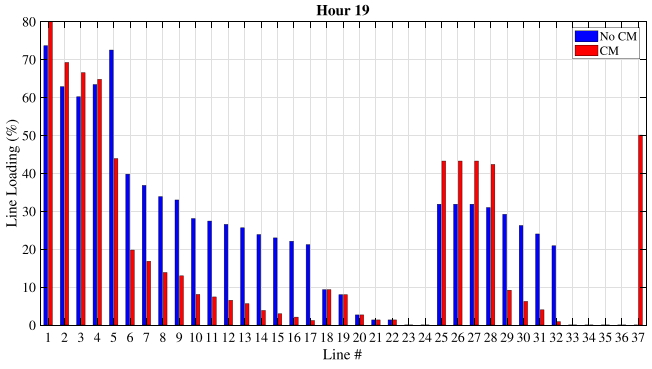

Fig. 39. Line loadings without/with congestion management (CM) at hour 19 in ***CS4***.

Table 7
Optimal switching of the ISO in ***CS2***.

Time	Open switches	Time	Open switches
1	12-22, 9-15, 8-21, 18-33, 25-29	13	12-22, 9-15, 8-21, 18-33, 25-29
2	12-22, 9-15, 8-21, 18-33, 25-29	14	12-22, 9-15, 8-21, 18-33, 25-29
3	12-22, 9-15, 8-21, 18-33, 25-29	15	12-22, 9-15, 8-21, 18-33, 24-25
4	12-22, 9-15,16-17, 8-21, 25-29	16	12-22, 9-15, 8-21, 26-27, 24-25
5	12-22, 9-15,16-17, 8-21, 25-29	17	12-22, 9-15, 8-21, 26-27, 24-25
6	12-22, 9-15, 8-21, 18-33, 25-29	18	12-22, 9-15, 8-21, 26-27, 24-25
7	12-22, 9-15, 8-21, 18-33, 25-29	19	12-22, 9-15, 8-21, 26-27, 24-25
8	12-22, 9-15, 8-21, 18-33, 25-29	20	12-22, 9-15, 8-21, 26-27, 24-25
9	12-22, 9-15, 8-21, 18-33, 25-29	21	12-22, 9-15, 8-21, 18-33, 25-29
10	12-22, 9-15, 8-21, 18-33, 25-29	22	12-22, 9-15, 8-21, 18-33, 25-29
11	12-22, 14-15, 8-21, 18-33, 25-29	23	12-22, 9-15, 8-21, 18-33, 25-29
12	12-22, 9-15, 8-21, 18-33, 25-29	24	12-22, 9-15, 8-21, 18-33, 25-29

The output of the optimization for thermal units such as P2HT, TES units and operation of fuel cells and also utility thermal transactions beside the energy level of the TESs, are shown in Fig. 26. Fuel cell consumption depends on all of electrical, thermal and hydrogen prices. According to the figure, the fuel cell usages has occurred between 15:00 to 23:00. They transform the stored hydrogen in HSS into electricity and thermal energy. Figs. 27 and 28 present the HSS scheduling for the VESS. In Fig. 27 optimal electric power generation/consumption of the fuel cells and electrolyzers beside P2HT units are shown. Electrolyzers use electrical energy to extract hydrogen from water and store the HSS tank. As mentioned before, fuel cells are interfacing units between all three carriers of energy. In these figures, interconnectivity of hydrogen, thermal and electrical carriers are shown. The interfacing units are fuel cells, electrolyzers and P2HT units. For instance, fuel cells generate electrical and thermal power at hour 17:00, due to their higher price. Meanwhile at hour 5:00, both electrolyzers and P2HT units consume electrical energy to produce thermal energy and hydrogen because of their higher price of hydrogen compared to electricity.

Table 8
Optimal switching of the ISO in ***CS3***.

Time	Open switches	Time	Open switches
1	12-22, 9-15, 8-21, 18-33, 25-29	13	12-22, 9-15, 8-21, 18-33, 25-29
2	12-22, 9-15, 8-21, 18-33, 25-29	14	12-22, 9-15, 8-21, 18-33, 25-29
3	12-22, 9-15, 8-21, 25-29, 29-30	15	12-22, 9-15, 8-21, 18-33, 25-29
4	12-22, 9-15, 8-21, 25-29, 29-30	16	5-6, 12-22, 9-15, 8-21, 25-29
5	12-22, 9-15, 8-21, 25-29, 29-30	17	12-22, 9-15, 8-21, 18-33, 25-29
6	12-22, 9-15, 8-21, 18-33, 25-29	18	12-22, 9-15, 8-21, 24-25, 25-29
7	12-22, 9-15, 8-21, 27-28, 25-29	19	12-22, 9-15, 8-21, 24-25, 25-29
8	12-22, 9-15, 8-21, 18-33, 25-29	20	12-22, 9-15, 8-21, 18-33, 25-29
9	12-22, 9-15, 8-21, 18-33, 25-29	21	12-22, 9-15, 8-21, 18-33, 25-29
10	12-22, 9-15, 8-21, 18-33, 25-29	22	12-22, 9-15, 8-21, 18-33, 25-29
11	12-22, 9-15, 8-21, 18-33, 25-29	23	12-22, 9-15, 8-21, 24-25, 25-29
12	12-22, 9-15, 8-21, 18-33, 25-29	24	12-22, 9-15, 8-21, 18-33, 25-29

Figs. 29 and 30, stand for voltage magnitude of the buses and line loadings at 19:00. These figures show a reduction in line loading, and the switching results are listed in Table 8.

4.4. CS4

In this case study, all the entities of VESS are included. Figs. 31–37 depict the optimization mean value results for different energy carriers. In this case study, the total revenue achieved by the VESS owner during 24-hour horizon is $3119 (see Table 8).

In this case, considering all the available VESS operational tools could gain more profit compared to other case studies. Figs. 31 and 32 illustrate the electrical power transactions of batteries. EVs utility and the SoC. With respect to figures, the batteries are charged during low price hours and discharged in high price periods. Further, the power has sold to the utility grid during the expensive hours, and participated in the VESS energy management during the other operational periods to gain higher profits. In addition, the batteries are fully discharged during 18:00–19:00. This is due to higher electrical energy prices, which motivates the VESS operator to completely use the stored energy in its units to sell to the consumers.

Optimal thermal power of the fuel cells, P2HT, TES units, utility transactions and energy level of the TESs, are shown in Fig. 33 to maximize the benefit. In Fig. 34, electric generation/consumption of fuel cell, electrolyzer and P2HT units are shown. During the early hours of the day, the electricity price is lower, and electrolyzer and P2HT units have consumed electrical energy to produce thermal power and hydrogen. In higher electricity prices, fuel cell has consumed hydrogen and generated electricity. The curves for hydrogen is shown in Fig. 35, which is also associated with Fig. 34, while presenting the hydrogen generation/consumption of different units are shown.

Table 9
Optimal switching of the ISO in ***CS4***.

Time	Open switches	Time	Open switches
1	12-22, 9-15, 8-21, 18-33, 25-29	13	12-22, 9-15, 8-21, 18-33, 25-29
2	2-3, 12-22, 9-15, 8-21, 25-29	14	12-22, 9-15, 8-21, 18-33, 25-29
3	12-22, 9-15, 8-21, 18-33, 25-29	15	24-25,12-22, 9-15, 8-21, 18-33
4	12-22, 9-15, 8-21, 18-33, 25-29	16	24-25,12-22, 9-15, 8-21, 18-33
5	12-22, 9-15, 8-21, 18-33, 25-29	17	24-25,12-22, 9-15, 8-21, 18-33
6	13-14, 12-22, 9-15, 8-21, 25-29	18	24-25,12-22, 9-15, 8-21, 18-33
7	13-14, 12-22, 9-15, 8-21, 25-29	19	24-25,12-22, 9-15, 8-21, 18-33
8	12-22, 9-15, 8-21, 18-33, 25-29	20	12-22, 9-15, 8-21, 18-33, 25-29
9	12-22, 9-15, 8-21, 18-33, 25-29	21	12-22, 9-15, 8-21, 18-33, 25-29
10	13-14, 12-22, 9-15, 8-21, 25-29	22	12-22, 9-15, 8-21, 18-33, 25-29
11	31-32, 12-22, 9-15, 8-21, 25-29	23	12-22, 9-15, 8-21, 18-33, 25-29
12	12-22, 9-15, 8-21, 18-33, 25-29	24	12-22, 9-15, 8-21, 18-33, 25-29

Table 10
Revenue of the VESS in various case studies.

Case study	***CS1***	***CS2***	***CS3***	***CS4***
Revenue ($)	2,781	892	2,927	3,119

Figs. 36 and 37 show the demand response results for both thermal and electrical demands. In fact, responsive loads are operated similar to the ESSs and a reduction is shown in higher price period, while an increment is shown in lower price hours. Further, afternoon hours are higher price periods, which show a step down for the flexible loads, and early morning hours show a step up for the electrical demands. Consequently, late night hours present a reduction for thermal loads due to their higher thermal energy price.

From the congestion management point of view, Figs. 38 and 39 show voltage magnitude of the buses and line loadings at 19:00. These figures depict that voltage variations are fluctuating between 1.02 p.u. and 0.9 p.u. Further, the congestion management shows a significant drop in line loadings mostly at the scheduling periods, and Table 9 represents the switching results.

4.5. Comparison of the results in various case studies

This subsection describes the financial results of the four case studies as shown in Table 10 for a comparative understanding of the various case studies, and the effect of operation of various technologies and carriers. The results confirm that the benefit of the VESS due to the insufficient thermal carrier is $2781, the VESS is benefited $892 by ignoring the hydrogen system. Finally, the benefit of the VESS becomes $2927 by neglecting DRP. Ultimately, considering all the units, the profit reaches to $3119. Accordingly, due to higher prices of hydrogen, it has the most effect on the VESS profit. The least effect on the revenue is created by DRP, however, it has the lowest investment cost. In all case studies, the congestion management has been efficiently performed.

5. Conclusion

Virtual Energy Storage Systems (VESSs) are one of the significant emerging concepts in modern smart grids. In fact, VESSs are accompanied with different energy storage systems to store the surplus energy and inject power during the power shortages according to the system requirements and the energy prices. Therefore, this study investigates the optimal operation of VESS in a multi-carrier energy system, while proposing a congestion management system to answer the rapid growth of power demand. Further, the problem is formulated as a bi-level model, where the upper level is controlled by ISO to resolve the congestion issues and the lower level is managed by VESS to maximize the benefits. The problem has been linearized to transform the bi-level problem into single level to obtain a global optima. Moreover, four case studies were considered where in the first, second and third cases have neglected one unit in the VESS, while in the fourth case all the units have been applied. The results confirm that, neglecting the thermal carrier, hydrogen system and DRP, the benefit of the VESS are $2781, $892 and $2927, respectively, while considering all the units, the profit has increased to $3119. Therefore due to higher prices of hydrogen, it has the most effect on the revenue of the VESS. On the other hand, although the DRP has the least impact, it has the lowest investment cost. In addition, an optimal switching action is performed in a reconfigurable network to manage congestion, which shows a reduction in line loadings. Overall, the results verify that the proposed system is benefited in both financially and technically. For future works, it is suggested to consider various sources of uncertainties in the optimization procedure such as renewable energy resources, demand levels, EV behaviors, etc. Also, a co-optimization of VESS owner, generation units in the network and ISO, each as a different agent and also participation in various markets such as real-time markets would be considered.

CRediT authorship contribution statement

Farid Hamzeh Aghdam: Conceptualization, Methodology, Validation, Formal analysis, Data curation, Writing – Original Draft, Visualization. **Manthila Wijesooriya Mudiyanselage:** Writing – review & editing, Visualization. **Behnam Mohammadi-Ivatloo:** Conceptualization, Methodology, Validation, Formal analysis, Visualization, Supervision. **Mousa Marzband:** Conceptualization, Methodology, Validation, Formal analysis, Visualization, Supervision.

Data availability

No data was used for the research described in the article.

Acknowledgments

This research is supported by the research grant of the University of Tabriz (number 1744). This work was supported from DTE Network+ funded by EPSRC grant reference EP/S032053/1.

References

[1] Luo X, Wang J, Dooner M, Clarke J. Overview of current development in electrical energy storage technologies and the application potential in power system operation. Appl Energy 2015;137:511–36.
[2] Savrun MM, İnci M. Adaptive neuro-fuzzy inference system combined with genetic algorithm to improve power extraction capability in fuel cell applications. J Clean Prod 2021;299:126944.
[3] Pan G, Gu W, Lu Y, Qiu H, Lu S, Yao S. Accurate modeling of a profit-driven power to hydrogen and methane plant toward strategic bidding within multi-type markets. IEEE Trans Smart Grid 2020;12(1):338–49.
[4] Lekvan AA, Habibifar R, Moradi M, Khoshjahan M, Nojavan S, Jermsittiparsert K. Robust optimization of renewable-based multi-energy micro-grid integrated with flexible energy conversion and storage devices. Sustainable Cities Soc 2021;64:102532.
[5] Felseghi R-A, Carcadea E, Raboaca MS, Trufin CN, Filote C. Hydrogen fuel cell technology for the sustainable future of stationary applications. Energies 2019;12(23):4593.
[6] Cinti G, Bidini G, Hemmes K. Comparison of the solid oxide fuel cell system for micro CHP using natural gas with a system using a mixture of natural gas and hydrogen. Appl Energy 2019;238:69–77.
[7] Mansour-Saatloo A, Ebadi R, Mirzaei MA, Zare K, Mohammadi-Ivatloo B, Marzband M, et al. Multi-objective IGDT-based scheduling of low-carbon multi-energy microgrids integrated with hydrogen refueling stations and electric vehicle parking lots. Sustainable Cities Soc 2021;74:103197.
[8] Khalatbarisoltani A, Kandidayeni M, Boulon L, Hu X. Power allocation strategy based on decentralized convex optimization in modular fuel cell systems for vehicular applications. IEEE Trans Veh Technol 2020;69(12):14563–74.
[9] Cheng M, Sami SS, Wu J. Virtual energy storage system for smart grids. Energy Procedia 2016;88:436–42.
[10] National Infrastructure Commission. Smart Power. UK Gov; 2016.
[11] Oh E. Risk-based virtual energy storage system service strategy for prosumers. Appl Sci 2021;11(7):3020.
[12] Pillay A, Karthikeyan SP, Kothari D. Congestion management in power systems–a review. Int J Electr Power Energy Syst 2015;70:83–90.

[13] Chung H-M, Su C-L, Wen C-K. Dispatch of generation and demand side response in regional grids. In: 2015 IEEE 15th international conference on environment and electrical engineering. EEEIC, IEEE; 2015, p. 482–6.
[14] Conejo AJ, Carrión M, Morales JM, et al. Decision making under uncertainty in electricity markets. vol. 1, Springer; 2010.
[15] Heitsch H, Römisch W. Scenario reduction algorithms in stochastic programming. Comput Optim Appl 2003;24(2):187–206.
[16] Zhao D, Wang H, Huang J, Lin X. Virtual energy storage sharing and capacity allocation. IEEE Trans Smart Grid 2019;11(2):1112–23.
[17] Zhong W, Xie K, Liu Y, Yang C, Xie S, Zhang Y. Online control and near-optimal algorithm for distributed energy storage sharing in smart grid. IEEE Trans Smart Grid 2019;11(3):2552–62.
[18] Jin X, Mu Y, Jia H, Wu J, Jiang T, Yu X. Dynamic economic dispatch of a hybrid energy microgrid considering building based virtual energy storage system. Appl Energy 2017;194:386–98.
[19] Cheng M, Sami SS, Wu J. Benefits of using virtual energy storage system for power system frequency response. Appl Energy 2017;194:376–85.
[20] Wang D, Meng K, Gao X, Qiu J, Lai LL, Dong ZY. Coordinated dispatch of virtual energy storage systems in LV grids for voltage regulation. IEEE Trans Ind Inf 2017;14(6):2452–62.
[21] Oh E, Son S-Y. Dynamic virtual energy storage system operation strategy for smart energy communities. Appl Sci 2022;12(5):2750.
[22] Kumar S, Krishnasamy V, Kaur R, Kandasamy NK. Virtual energy storage-based energy management algorithm for optimally sized DC nanogrid. IEEE Syst J 2021;16(1):231–9.
[23] Chen C, Deng X, Zhang Z, Liu S, Waseem M, Dan Y, et al. Optimal day-ahead scheduling of multiple integrated energy systems considering integrated demand response, cooperative game and virtual energy storage. IET Gener Transm Dist 2021;15(11):1657–73.
[24] Zhu X, Yang J, Liu Y, Liu C, Miao B, Chen L. Optimal scheduling method for a regional integrated energy system considering joint virtual energy storage. Ieee Access 2019;7:138260–72.
[25] Kang W, Chen M, Li Q, Lai W, Luo Y, Tavner PJ. Distributed optimization model and algorithms for virtual energy storage systems using dynamic price. J Clean Prod 2021;289:125440.
[26] Kang W, Chen M, Lai W, Luo Y. Distributed real-time power management for virtual energy storage systems using dynamic price. Energy 2021;216:119069.
[27] Niromandfam A, Pour AM, Zarezadeh E. Virtual energy storage modeling based on electricity customers' behavior to maximize wind profit. J Energy Storage 2020;32:101811.
[28] Aghdam FH, Kalantari NT, Mohammadi-Ivatloo B. A chance-constrained energy management in multi-microgrid systems considering degradation cost of energy storage elements. J Energy Storage 2020;29:101416.
[29] Tan S, Xu J-X, Panda SK. Optimization of distribution network incorporating distributed generators: An integrated approach. IEEE Trans Power Syst 2013;28(3):2421–32.
[30] Ghaemi S, Salehi J, Aghdam FH. Risk aversion energy management in the networked microgrids with presence of renewable generation using decentralised optimisation approach. IET Renew Power Gener 2019;13(7):1050–61.
[31] Jabr RA, Singh R, Pal BC. Minimum loss network reconfiguration using mixed-integer convex programming. IEEE Trans Power Syst 2012;27(2):1106–15.
[32] Jadhav AM, Patne NR. Priority-based energy scheduling in a smart distributed network with multiple microgrids. IEEE Trans Ind Inf 2017;13(6):3134–43.
[33] Dupacová J, Gröwe-Kuska N, Römisch W. Scenario reduction in stochastic programming: An approach using probability metrics. Humboldt-Universität zu Berlin, Mathematisch-Naturwissenschaftliche Fakultät; 2000.
[34] Ghaemi S, Salehi J, Moeini-Aghtaie M. Developing a market-oriented approach for supplying flexibility ramping products in a multimicrogrid distribution system. IEEE Trans Ind Inf 2020;17(10):6765–75.